Politecnico di Torino

POLITECNICO DI TORINO

Master's degree in Biomedical Engineering
Academic year 2023/2024

Fabrication and analysis of GelMA-based hydrogel strain sensors for wearable applications

Supervisor	Candidate
Prof. Stefano STASSI	Marco FERRANTE

JULY 2024

Abstract

In recent years, the development of wearable biomedical sensors based on GelMA (Gelatin Methacryloyl) has sparked significant interest due to their potential to revolutionize healthcare monitoring. GelMA, derived from gelatin, is a biocompatible hydrogel with versatile properties that make it highly suitable for integration into wearable sensor technologies.

These sensors are very useful for GelMA's biocompatibility, ensuring minimal adverse reactions when in contact with biological tissues, thereby supporting long-term wearability. Furthermore, GelMA can be tailored by incorporating additives to enhance its electrical conductivity, mechanical strength, and overall durability. This enhancement enables the sensors to accurately detect and transmit vital physiological data, encompassing parameters such as heart rate, respiratory rate, motion, and environmental conditions.

The integration of GelMA into wearable sensors addresses the demand for devices that are lightweight, flexible, and comfortable for continuous use. This technological advancement holds promise across various healthcare applications, including remote patient monitoring, sports performance analysis, and rehabilitation tracking.

This thesis specifically focuses on advancing a GelMA-based conductive hydrogel sensor through the incorporation of additives aimed at improving its electrical, mechanical, and durability properties, while maintaining biocompatibility. The addition of glycerol and citric acid has yielded promising results. Cytocompatibility, deformation, and electrical tests were conducted to thoroughly characterize the material. The sensor has demonstrated modest sensitivity in detecting minor deformations. Additionally, it demonstrated satisfactory mechanical strength, excellent stability, a low limit of detection, and rapid response times. These findings suggest that these sensors could serve as a promising foundation for developing biomedical devices that are easy to wear, comfortable, and safe, without compromising patient activities or causing adverse tissue reactions.

Table of Contents

List of Figures III

1 Introduction 1
- 1.1 Regenerative Medicine . . . 1
- 1.2 Biomedical Sensors . . . 5
  - 1.2.1 GelMA-based sensors . . . 7

2 Hydrogel 11
- 2.1 Definition and classification . . . 11
- 2.2 Physical crosslinking . . . 15
  - 2.2.1 Hydrophobic interactions . . . 15
  - 2.2.2 Electrostatic interactions . . . 16
  - 2.2.3 Crystallization . . . 17
  - 2.2.4 Hydrogen bonding . . . 17
  - 2.2.5 Stereocomplexation . . . 18
- 2.3 Chemical crosslinking . . . 19
  - 2.3.1 Photopolymerization . . . 19
  - 2.3.2 Enzymatic cross-linking . . . 22
  - 2.3.3 Smart hydrogel . . . 22
- 2.4 Hydrogel strain sensors . . . 23
  - 2.4.1 Piezoresistive sensor . . . 25
  - 2.4.2 Capacitive sensors . . . 26
  - 2.4.3 Piezoelectric sensors . . . 28
  - 2.4.4 Triboelectric sensors . . . 29
  - 2.4.5 Ionic-conductive hydrogel sensors . . . 29

3 Materials and methods 31
- 3.1 GelMA-based hydrogel synthesis . . . 31
  - 3.1.1 GelMA synthesis . . . 31
  - 3.1.2 Hydrogel synthesis . . . 33
- 3.2 Material characterization . . . 37

3.2.1 Degree of methacrylation using formaldehyde (DOF) 37
3.2.2 Citocompatibility test 39
3.3 Hydrogel and sensor characterization 40
3.3.1 % Gel 40
3.3.2 FTIR-ATR spectroscopy 41
3.3.3 Tensile and compression test 42
3.3.4 Electrical test 44

4 Results and discussion 45
4.1 Material characterization 45
4.1.1 Degree of methacrylation using formaldehyde (DOF) 45
4.1.2 Citocompatibility test 45
4.2 Hydrogel and sensor characterization – Impact of Citric Acid 48
4.2.1 % Gel 48
4.2.2 FTIR-ATR spectroscopy 48
4.2.3 Tensile and electrical tests 50
4.2.4 Temperature dependency of resistance 55
4.3 Hydrogel and sensor characterization – Impact of Tannic Acid . . . 55

5 Conclusions 59

Bibliography 64

List of Figures

1.1 Stem cells in regenerative medicine . . . 2
1.2 Exemple of chemical structure of gelatin . . . 3
1.3 Production of a GelMA-CA hydrogel-coated pancreatic stents . . . 5
1.4 Exemples of biosensors . . . 6
1.5 Biodegradable piezoelectric PLLA pressure sensor . . . 6
1.6 Fabrication process of the GelMA-CA-Gly hydrogel . . . 7
1.7 Schematic illustration of magnetic-based strain sensor . . . 8
1.8 Schematic illustration of the structure of GelMA-PDMS hydrogel-based pressure sensors . . . 8
1.9 Schematic illustration of the LMGE and its manufacturing process . 9
1.10 Self-healing ability of PPy-GelMA-Fe hydrogel . . . 9
1.11 GelMA-TA hydrogel . . . 10
1.12 Strain Test of Gelatin-CA-Glycerol hydrogel . . . 10

2.1 SEM images of GelMA hydrogel . . . 11
2.2 Swelling in a drug delivery hydrogel . . . 14
2.3 Hydrophobic interactions . . . 15
2.4 Electrostatic interaction . . . 16
2.5 Hydrogen bond . . . 18
2.6 Free radical photopolymerization . . . 20
2.7 LAP . . . 21
2.8 TPO . . . 22
2.9 Enzymatic crosslinking method . . . 23
2.10 Mechanical properties of different hydrogels . . . 25
2.11 Change in electrical resistance of a piezoresistive sensor that occur when a material is deformed . . . 26
2.12 Change in capacitance of a capacitive sensor that occur when a pressure is applied . . . 27
2.13 Change in electrical impulse of a piezoelectric sensor that occur when a deformation is applied . . . 28

3.1 Scheme of the reactions for the synthesis of GelMA 32
3.2 Experimental setup used for GelMA synthesis 32
3.3 Dialysis of GelMA 33
3.4 Preparation of lyophilized GelMA and desiccated GelMA 33
3.5 Experimental setup used for GelMA-based hydrogel synthesis 34
3.6 GelMA-in-water solubilization process 35
3.7 Experimental setup used for hydrogel preparation 36
3.8 Scheme of the reactions for the crosslinking of GelMA 37
3.9 Preparation of the (2mL)-Eppendorf microtubes 38
3.10 Preparation of the laboratory plate 39
3.11 Example illustrating how the results are displayed in the software . 39
3.12 %Gel method 41
3.13 Tensile test 43
3.14 Compression test 43
3.15 Electrical test 44

4.1 Different colour of the medium 46
4.2 Live/dead assay used to assess cell viability 47
4.3 Results of the MTT assay 47
4.4 Table of %Gel results in samples without citric acid 48
4.5 Table of %Gel results in samples with 20% w/w citric acid 48
4.6 FTIR-ATR spectroscopy results - CA 49
4.7 Compression curves of samples with CA 51
4.8 Tensile tests to failure of samples with CA 51
4.9 Durability test for 70 days on different samples 52
4.10 Stress-strain curve between the sample without citric acid and with 30% and 50% w/w of citric acid 53
4.11 $\Delta R/R$-time and $\Delta C/C$-time curves of samples without citric acid and with 30% and 50% w/w of citric acid 54
4.12 The variation of resistance on sample without citric acid 56
4.13 The variation of resistance on sample with different concentration of citric acid 56
4.14 Dimensions and resistance of samples immersed in tannic acid solution for different time 57
4.15 FTIR-ATR spectroscopy results - TA 58
4.16 FTIR-ATR spectroscopy results - 15h TA 58

5.1 FINGER BENDING – Resistance and capacitance signal in reaction to different bending angles 61
5.2 Vocal cord vibrations detection, hand bending monitoring, and finger bending monitoring 61

Chapter 1

Introduction

The integration of technology with the human body is rapidly evolving, and hydrogels are emerging as key components in the field of sensors for wearable applications. Hydrogels are polymer materials known for their ability to absorb and retain large amounts of water, offering elasticity and softness similar to that of biological tissues. This makes hydrogels particularly suitable for creating strain sensors, devices capable of detecting changes in mechanical stresses such as stretches and compressions. These hydrogel strain sensors have multiple applications in wearable devices, contributing to real-time monitoring of body movements and functions for medical, sports, or safety purposes. The adaptability and sensitivity of these sensors allow for accurate measurements, providing a comfortable and safe user experience. In this thesis, we will examine the design and fabrication process of hydrogel strain sensors based on GelMA for wearable applications. We will look at fabrication techniques, challenges associated with their implementation, and potential applications. The goal is to explore how these innovative sensors are shaping the future of wearable technology and health monitoring.

1.1 Regenerative Medicine

The multidisciplinary discipline of regenerative medicine uses concepts from biology and engineering to encourage the regeneration of tissues and organs. By restoring damaged and sick tissues as well as entire organs, it seeks to reduce the need for organ transplants. This field includes FDA-approved treatments for wound healing and orthopedics, among others. It also investigates preclinical and clinical environments for the development of complex grafts, tissue mimics, and technologies for graft integration with host vasculature. It entails taking advantage of recently created cell sources and boosting the host's natural ability to regenerate through techniques like immune modulation or cell infusions [1]. The use of stem cells is another

aspect of regenerative medicine; these cells are essential since they have the ability to self-renew endlessly and specialize into a variety of cells. Promising outcomes from stem cell research have been observed in several fields, including induced pluripotent stem cells (iPSCs), bone marrow stem cells (BMSCs), umbilical cord stem cells (UCSCs), mesenchymal stem cells (MSCs), and tissue-specific progenitor stem cells (TSPSCs). In order to transform stem cells ex vivo into 3D organoids and tissue architectures for individualized applications, this research makes use of developments in tissue engineering and gene editing. It has a wide range of uses, including the treatment of serious wounds, long-term illnesses, and possible use in the preservation of wildlife [2].

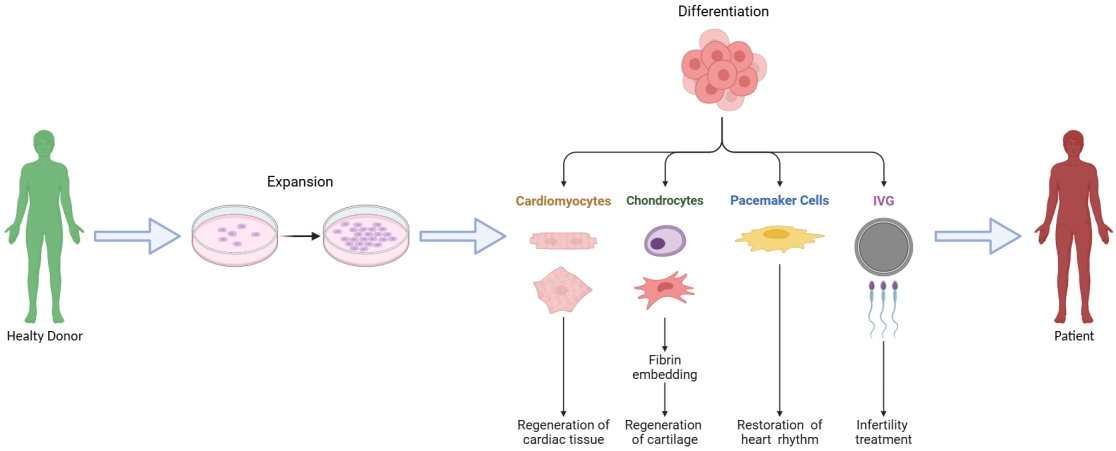

Figure 1.1: Stem cells in regenerative medicine. Stem cells are extracted from the healthy donor, they are proliferated, and subsequently differentiated through physical stimuli or chemical/environmental conditions; finally, the cells are implanted into the patient.

Furthermore, the use of human somatic cells, adult stem, or embryo-derived cells defines regenerative medicine. It has developed from a range of medical procedures and innovations, such as tissue engineering, organ transplants, and surgery. The goal of the area is to get past the drawbacks of conventional medical interventions, like the requirement for immunosuppressive medications during organ transplants or the inflammatory reactions brought on by artificial tissue scaffolds [3].

Biopolymer in Regenerative Medicine

A large molecule made up of naturally occurring repeating structural components called monomers is referred to as a natural polymer. Natural sources such as plants, animals, and microorganisms provide these polymers. Natural polymers are widely accepted as natural materials in regenerative medicine due to their inherent

bioactivities. These materials are crucial in regenerative medicine because they can be modified to enhance their bioactivities, which is essential for advancing the field. The development of these materials and the understanding of their composition/-function relationships can significantly improve tissue regeneration processes. In addition, the other reasons for which they are used are the high biocompatibility, the biodegradability and the tunability, i.e. they can be adjusted to resemble the intended target tissue more closely [4]. Based on their chemical makeup, natural polymers can be divided into three main groups: polysaccharides, proteins, and polyesters [5]. Natural proteins will be the focus of this thesis. A natural protein is a biological macromolecule made up of amino acids that are essential to the composition, operation, and control of living things' cells and tissues. They are widely distributed and essential for the growth, development, and upkeep of living things and they can be found in a wide range of sources, such as plant seeds, animal tissues, and microbes. Some examples of protein are collagen, keratin, albumin, and myosin [6].

Gelatin Methacryloyl (GelMA) in Regenerative Medicine

Gelatin [Fig. 1.2] is derived from collagen, a protein found in mammalian skin, tendons, connective tissue, ligaments, and bones. Usually, it comes from materials like fish scales, pig skin, cow bones, and infrequently, plant-based alternatives. Gelatin, which is well-known for its gelling properties, is widely used in the food industry as well as a variety of other industries, such as medicines, cosmetics, and biomedical engineering [6].

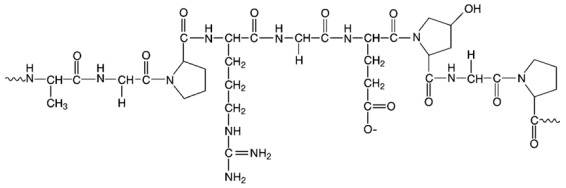

Figure 1.2: Exemple of chemical structure of gelatin[1]

Gelatin Methacryloyl, or GelMA, is a gelatin derivative that is produced by a chemical reaction in which the methacrylic anhydride (MA) binds to the amino groups (NH_2) of the gelatin. Gelatin contains various functional groups derived from the amino acids that make up it, but amino groups (NH_2) in the lateral chain of amino acids such as lysine or hydroxylysine are the main reaction sites. This change gives GelMA a variety of uses and characteristics like excellent mechanical

[1]Gelatin Nanoparticles and Their Biofunctionalization - Scientific Figure on ResearchGate

and electrical properties, which makes it an extremely adaptable material for use in biomedical research and applications [7]. The main applications of GelMA are tissue engineering (to produce bio-printed scaffolds, 3D scaffolds and membranes), wound healing (potential to function as wound dressings, hasten the healing process, and encourage the development of cutaneous tissues and multilayered epidermis) and biosensing (wearable strain sensors and stress sensors) [7]. Using GelMA has the following primary benefits:

- Structural integrity: aids in giving the hydrogels structural integrity so they can keep their shape and promote the growth and proliferation of cells.
- Biocompatibility: since collagen is a naturally occurring protein, gelatin methacryloyl is biocompatible and safe to use in biological systems without producing negative side effects.
- Modifiable properties: gelMA can be made to have adjustable mechanical strength and rates of degradation to meet certain tissue engineering requirements.
- Crosslinking ability: gelatin methacryloyl can build stable hydrogel networks that can encase cells and bioactive compounds by crosslinking it with other materials through techniques like UV irradiation [8].

Over the years, GelMA has been increasingly used and investigated. Jirong Yang et al. in their study discuss about a mechanical-assisted post-bioprinting strategy for bone repair using heart-inspired hollow hydrogel-based scaffolds (HHSs), showcasing promising results in regenerative therapy. These hydrogels, made of a combination of gelatin methacryloyl, laponite nanoclay and N-acryloyl glycinamide, show rapid shape recovery, and exceptional fatigue resistance; making possible the repairing of osteoporotic bone defects in vivo [8]. Jo, S., Lee, J., Lee, H. et al. demonstrated the successful synthesis of GelMA structures loaded with human antenatal stem cells, highlighting the potential of this technique for muscle regeneration. In the work, pharmacological and biophysical stimuli were included into the culture of human adipose stem cells (hASCs) within GelMA structures. The two types of bioinks that were used were the porous bioink (experimental) and the hASC-GelMA bioink (control). These bioinks were placed in a mold and left to incubate [9]. The research projects done by Sattwikesh Paul et al. on highly adhesive GelMA-Glycol Chitosan Hydrogels that are injectable and photo-cross-linkable, find out that these hydrogels have excellent potential for cartilage repair applications. The investigation proved that these hydrogels had advantageous characteristics, including in vitro degradation, rheological characterization and cell survival. These hydrogels appear to be a potential choice for tissue regeneration and growth [10].
Studies conducted recently have demonstrated that GelMA hydrogel reinforced

with a coating of citric acid leads to increased mechanical strength and decreased swelling at higher concentrations of CA. Furthermore, this additive is naturally an excellent calcium chelator, making it an ideal body calculus remover. In an in vivo investigation, Jing Li et al. create a stent with a GelMA-CA coating [Fig. 1.3] and remove the calculi in three days, demonstrating also an excellent cytocompatibility and biodegradability of the material [11].

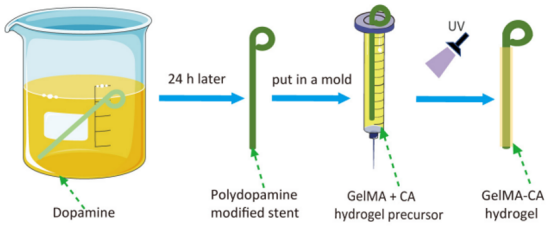

Figure 1.3: Production of a GelMA-CA hydrogel-coated pancreatic stents [11]

1.2 Biomedical Sensors

This thesis focuses on the development of biomedical sensor, a device capable of detecting, measuring, and transmitting information about various biological or physiological parameters of the human body, designed to produce varying outputs in response to changes in external conditions such as temperature, length, pressure and humidity.
For example, F. Khoshnoud et al.'s study on intramuscular pressure concluded that MEMS (micro-electromechanical systems) sensors are critical to the improvement of medical science and healthcare. The integration of MEMS sensors into a wide range of medical instruments and devices improves the accuracy and effectiveness of diagnostics and treatments. Chemicals including glucose, proteins, and triglycerides can be detected by MEMS-based biological sensors[Fig. 1.4]. They can also be used to measure tissue softness or provide surgical assistance through the use of robotic fingers with pressure sensors [12].
Since physical characteristics like radiation and pressure are vital for medical diagnosis, physical sensors are also being employed in healthcare more and more. In actuality, biological sensors have the potential to enhance people's quality of life by providing vital information for disease prevention, management, and treatment, as well as enhancing patient outcomes and the effectiveness of healthcare delivery [13].
In recent years, there has been a substantial advancement in sensor technology for biomedical applications. Implantable sensors, as emphasized by Yang Li et al., are an important area of focus in the realm of wearable and biodegradable sensors.

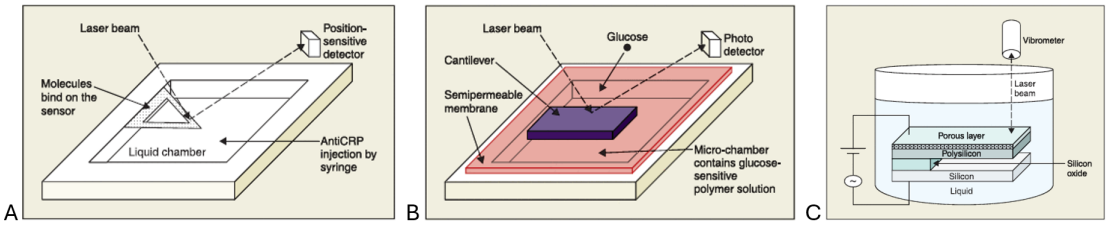

Figure 1.4: Exemples of biosensors. A) A triglyceride biosensor with a cantilever beam in liquid. B) A bio-MEMS sensor for C-reactive protein detection. and C) A MEMS affinity sensor for detection of glucose [12].

These sensors are intended to be implanted in the human body and are built of biocompatible and biodegradable materials to avoid unpleasant responses and to safely disintegrate after their effective lifetime. Implantable sensors are especially crucial for continuous, real-time monitoring of health conditions within the body, as they provide critical data for medical diagnoses and therapy monitoring [14]. Furthermore, according to Zhou et al.'s analysis, flexible sensors combine the distinct benefits of flexibility and cheap cost, which are critical for applications in high-performance electronic equipment and gadgets. Because of their elasticity, they can adapt to a wide range of surfaces and forms, which is particularly helpful for human-machine interactions, healthcare monitoring, and therapy. These sensors can detect a wide range of biological signals, such as gas molecules, small molecules, DNA/RNA[Fig. 1.5], and proteins. They are used in biomedical applications. They are very beneficial to the development of contemporary social science and technology because of this attribute [15].

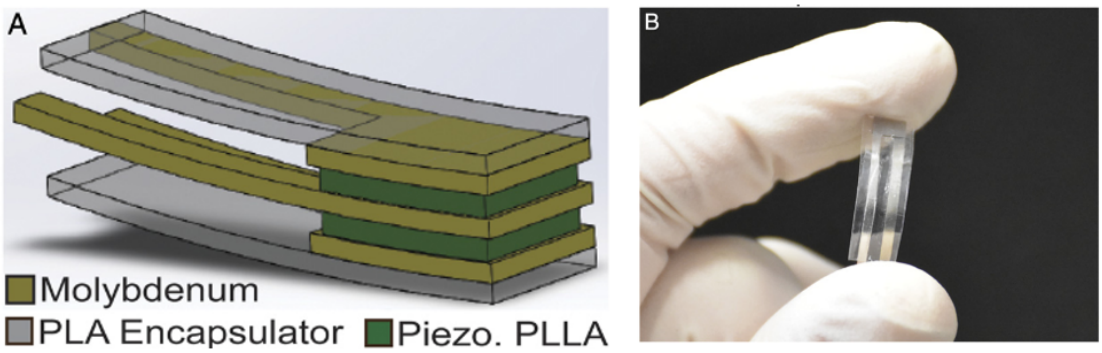

Figure 1.5: Biodegradable piezoelectric PLLA pressure sensor. A) Schematic representing the biodegradable sensor. B) A fabricated biodegradable piezoelectric sensor (5 mm $\times$ 5 mm x 200 μm) [16].

Another important additive that has been introduced in some studies was citric acid.

Baumgartner et al. developed a hydrogel with Gelatine, water, glycerol, citric acid and sodium chloride, demonstrating that the acidic environment created by a small amount of citric acid prevents bacteria from proliferating [17]. Hardman et al.ined the same materials as the above-mentioned study, modifying the concentrations of individual elements [Fig. 1.6], the result is a hydrogel with better mechanical properties, printability and stability, all these factors are dependent on the salt concentration inserted in the formulation [18].

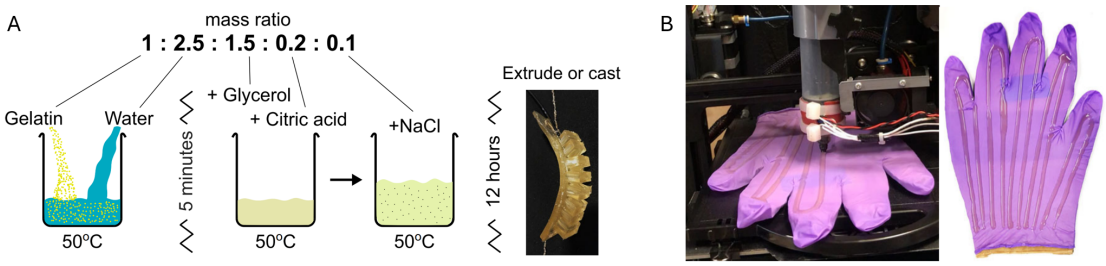

Figure 1.6: A) Fabrication process of the GelMA-CA-Gly hydrogel. B) Sensor printed directly on the surface of a nitrile glove [18].

The chapter underscore how sensor technology in biological applications is dynamic and ever evolving. Health monitoring and disease management are at the forefront of technological breakthroughs thanks to wearable, implantable, and flexible sensors. Modern materials and MEMS technology come together in these sensors, which are critical for accurate, real-time medical diagnosis and treatment.

1.2.1 GelMA-based sensors

As previously mentioned in chapter 1.1, GelMA is also used for the creation of biomedical sensors. Most of the proposed studies use a metal to enhance the conductive capabilities of the material, a crucial aspect when it comes to biomedical sensors. Another fundamental point regarding sensors is the detection limit, which is the smallest measurable variation; the goal is to make it as small as possible to detect even the slightest changes. The sensitivity (GF) is a factor calculated by dividing the change in output by the change in input. Generally, we always aim to achieve high sensitivity to be able to observe a significant variation in the variable we want to measure, even if the input variation is minimal.
Qi Zhang et al. studied magnetic field-based sensing devices for real-time and in-situ monitoring of physiological signals [Fig. 1.7]. This ensured a higher depth of penetration to detect signals compared to other sensors already on the market and greater resistance to ionic interferences. The devices are composed of a magnetic hydrogel film of gelatin methacryloyl ($GelMA/Fe_3O_4$) prepared with iron oxide

nanoparticles and subsequently cultured with cardiomyocytes to obtain an in vitro model of cardiac contraction [19].

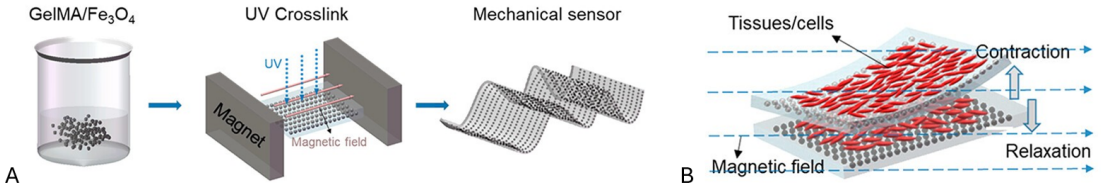

Figure 1.7: A) Schematic illustration of a magnetic-based strain sensor and B) Schematic working mechanism of an in vitro tissue model [19].

Zhikang Li et al. show a capacitive tactile sensor made of PDMS/GelMA/PDMS to create the dielectric layers and PEDOT for the electrodes. Through a strong chemical bond and an effective PDMS encapsulation layer, the sensor avoids water evaporation, a common problem in hydrogel biosensors. The pressure sensors under study exhibit better pressure sensitivity and higher limit of detection when compared to existing hydrogel sensors [Fig. 1.8]. In addition, they are extremely robust and stable over time. These features make them perfect for monitoring human physiological signals, making them ideal for wearable medical devices [20].

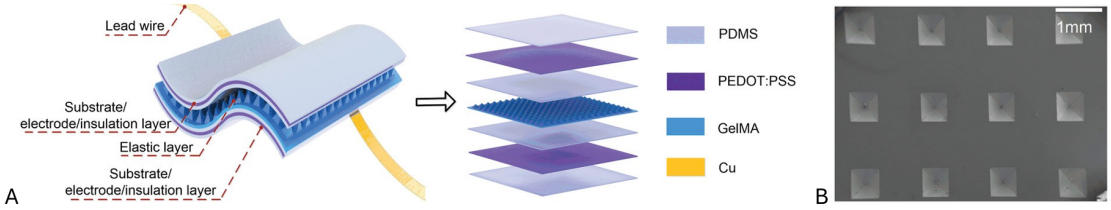

Figure 1.8: A) Schematic illustration of the structure of GelMA-PDMS hydrogel-based pressure sensors. B) SEM pictures of the pyramidal structure [20].

Yuan et al. investigate how GelMA can be used to make multifunctional wearable electronics by incorporating liquid metals into GelMA's hydrogel [Fig. 1.9], which improves their elasticity and biocompatibility. These GelMA hydrogel electronics with liquid metals (LMGE) have the ability to track physical movements and even heartbeats in rats. They can also wirelessly track human secretions while exercising. This development opens the way for integrated monitoring and biomedical applications thanks to the unique properties of GelMA combined with the conductivity and rheology of liquid metals [21].
Wang et al. talk about the creation of a gelatin-based hydrogel infused with polypirrol that has conductive, self-regenerating [Fig. 1.10] and injectable properties. These hydrogels are highly appreciated for their excellent conductivity because they are mixed with iron ions and this makes them essential for applications that

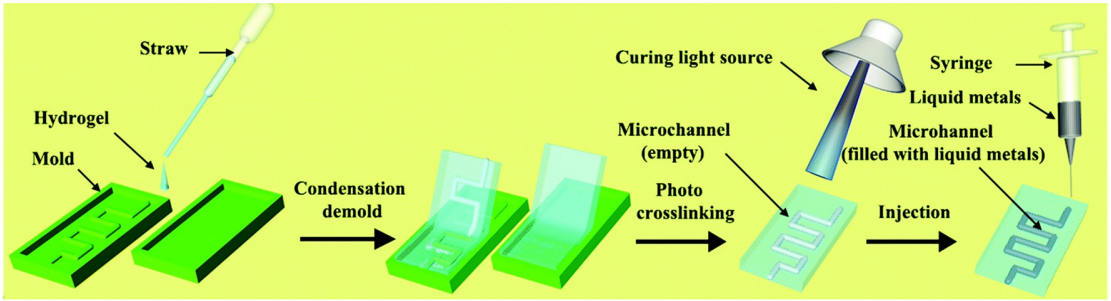

Figure 1.9: Schematic illustration of the LMGE and its manufacturing process [21].

require electrical stimuli, such as sensors. These hydrogels have the ability to self-regenerate, which indicates that they could be used to create sensor systems that will last long. The hydrogel also demonstrated a controllable porous structure, less swelling, and good cytocompatibility and compatibility with the blood [22].

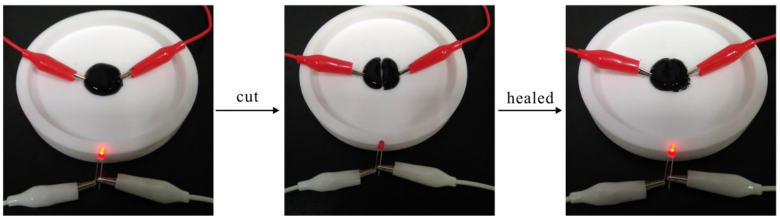

Figure 1.10: PPy-GelMA-Fe hydrogel's capacity of self-healing using a LED indicator circuit [22].

Liu et al. study a double-network (DN) hydrogel based on GelMA and reinforced with tannic acid and it demonstrate excellent properties of elasticity, self-regeneration, and self-adhesion underwater. These features are used to create a self-healing electrical skin with strain-sensitive conductivity, increasing the capacities by incorporating multiple-walled carbon nanotubes. Tannic acid (TA) is introduced into GelMA's hydrogel to enhance their mechanical properties, significantly increasing their compression module and tensile properties making them more flexible and resilient. TA also improves the adhesive properties of hydrogel at the price of a decrease in volume [Fig. 1.11]. Finally, cytocompatibility tests showed that the material was extremely biocompatible. Therefore, in vivo experiments have shown that GelMA-TA hydrogel worked well to close surgical incisions without suture on the skin and stomach tissue [23]. The tannic acid inside the hydrogel demonstrate a significant potential. GelMA-TA hydrogeles show a large increase in adhesiveness, mainly due to the presence of numerous polyphenol groups that generate dense cross-linking and strong tissue adhesion to many substrates where

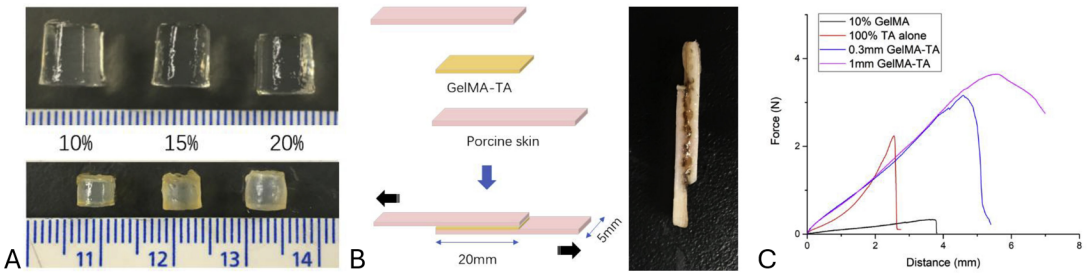

Figure 1.11: A) Morphological changes from GelMA hydrogels (upper) to GelMA-TA (bottom) after incubation in TA solution. B) Hydrogel adhesion test. C) Force-distance curves for hydrogels with 10% GelMA and fibrin glue, for hydrogels with 100% TA, for hydrogels with the thickness of 0.3 mm and 1 mm [23].

the adhesive properties are directly proportional to the concentration of TA [24]. As was previously mentioned [Chapter 1.1], Jing Li et al. created a GelMA-CA hydrogel that outperformed the traditional GelMA hydrogels in terms of mechanical properties. Specifically, the mechanical properties improved and the swelling decreased as the concentration of CA in the formulation increased [11]. Because of all of this, citric acid is a great ingredient to include in formulations to produce biomedical sensors that have better mechanical qualities. Furthermore, glycerol was included as the primary constituent of the formulation in the Hardman et al. study in addition to citric acid [Fig. 1.12]. This is a crucial component for a number of reasons:

- It is a non-solvent for gelatin;
- It is a plasticizer;
- Enhances moisture sensitivity, elasticity, and flexibility by minimizing interactions between neighboring gelatin chains;
- Both the hydrogel's stability and durability are increased [18].

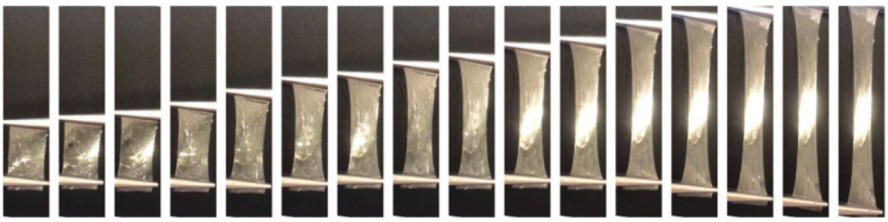

Figure 1.12: Strain Test of Gelatin-CA-Glycerol hydrogel [18].

Chapter 2

Hydrogel

2.1 Definition and classification

Hydrogels are 3D polymeric materials networks with various physical characteristics and high water content, in fact they have the capacity to absorb water up to hundreds of times its dry weight [25]. These structures are created by crosslinking natural or synthetic polymers physically or chemically, allowing them to swell in water, which is why they are also known as hydrophilic gels. Dried hydrogels are called "xerogels," and when dehydrated without disrupting their network, e.g. by lyophilization, they become "aerogels" with porosity as high as 98 percent [Fig.2.1] [26].

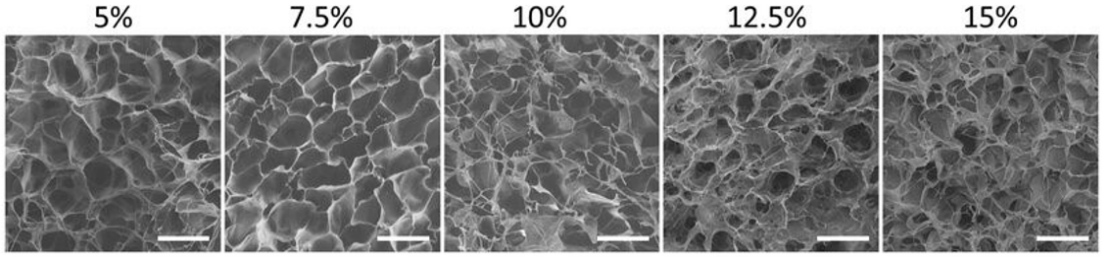

Figure 2.1: SEM images of GelMA hydrogel showing different pore sizes and shapes of each GelMA concentration [27].

Hydrogels can be divided into three groups: natural, synthetic, and semi-synthetic. Synthetic hydrogels differ from natural hydrogels in their large range of raw chemical resources, longer lifespan and increased water-absorbing capacity [28]. This is achieved with the unique chemical makeup and structure of the synthetic polymers employed in the preparation of the hydrogels, the chemical structure of synthetic hydrogels may be accurately regulated during their synthesis [28].

Synthetic hydrogels also have better mechanical qualities, because of their unique composition and design, synthetic hydrogels are more flexible than natural hydrogels. The fracture energy and stretchability of synthetic hydrogels have been found to be greatly enhanced by mixing weak and strong crosslinks. The hydrogels' remarkable mechanical qualities are demonstrated by their ability to be stretched more than 20 times their original length. Natural hydrogels, on the other hand, like alginate hydrogels, usually burst when stretched to a length that is around 1.2 times its initial length. Synthetic hydrogels have higher stretchability and durability than natural hydrogels due to the combined effects of covalent crosslinks that bridge cracks and hysteresis caused by unzipping the network of ionic crosslinks [29]. The final aspect is their well regulated degradation, compared to natural hydrogels, which may have more complex and stable structures, synthetic hydrogels are frequently manufactured with specific chemical compositions and architectures that make them more vulnerable to destruction by enzymes or other biological processes [30].

- **Natural hydrogels**: most naturally occurring hydrogels come from sources like proteins or polysaccharides that are present in living things. These natural polymers can produce hydrogel through ionic interactions, gelation or self-assembly. Natural hydrogels such as collagen, alginate and hyaluronic acid are great for biomedical applications because the body generally tolerates them well. These polymers' resemblance to naturally occurring biological structures allows them to facilitate both tissue regeneration and cell development. Natural polymers, on the other hand, may have batch-to-batch variability, lower mechanical strength when compared to synthetic polymers, and the potential for immunogenic reactions in some persons. The consistency of performance of natural polymers generated from biological sources may be impacted by differences in their composition and characteristics. Furthermore, natural polymers could not have as strong of mechanical qualities as synthetic polymers, which would restrict their usage in some applications that call for extreme durability or strength. Additionally, certain people may react immunologically to natural polymers, which might cause problems with biocompatibility [31].

- **Synthetic hydrogels**: are usually created by creating a three-dimensional network structure through the crosslinking of hydrophilic polymers. There are several ways to do this crosslinking, including chemical reactions, physical interactions, and radiation-induced processes. Hydrogels get their distinctive swelling behavior from the polymers' ability to absorb and hold onto water or biological fluids due to their hydrophilic nature. Some examples of synthetic polymer are Acrylic acid, Hydroxyethyl methacrylate (HEMA), Vinyl acetate and Methacrylic acid(MAA). Some advantages of synthetic hydrogels include their high water content at equilibrium, rubbery behavior, good

biocompatibility, and resemblance to natural tissues. These hydrogels are used in numerous biomedical applications, including ophthalmological devices, biosensors, biomembranes, and controlled drug delivery systems. The adaptability of synthetic polymers in terms of their chemical makeup and physical characteristics, which may be customized for certain uses, is another benefit. It is possible to engineer synthetic polymers to exhibit regulated release qualities, diffusion traits, and stimuli-responsive behavior. Slow dynamics, which may impact how quickly synthetic hydrogels react to outside stimuli, is one of their potential disadvantages. Hydrogels respond only when certain molecules diffuse into them; the amount of time needed for this diffusion depends on the hydrogel sample's size and the molecules' diffusion coefficient. One of the possible drawbacks of synthetic polymers could be their inability to accurately replicate the intricate structure and activity of real tissues. Even while synthetic polymers are more versatile in terms of their physical and chemical makeup, they might not always be able to perfectly mimic biological tissues' characteristics. Furthermore, the creation and synthesis of synthetic polymers for particular uses can be difficult and necessitate in-depth understanding of material science and polymer chemistry [31].

- **Semi-synthetic hydrogels**: it is advantageous to combine synthetic and natural polymers in biomaterials because this allows you to merge the best qualities of both kinds of materials to be included, like the ability to create stable and resilient formulations. These hydrogels are designed to mimic the extracellular matrix (ECM), which offer a regulated environment for cell function, especially in tissue engineering applications such as peripheral nerve regeneration. Other advantages of using semi-synthetic hydrogels include: the possibility of controlling cell behavior in response to biodegradation, mechanical characteristics, and biological traits; the assistance with glial cell migration and neurite extension during peripheral nerve regeneration; the control over characteristics that affect cell outgrowth, including as density and proteolytic breakdown; the possibility for scientific research on neuronal morphogenesis and nerve regeneration as well as for therapeutic product development in the treatment of severed nerve injury. For exemple the study by Yulia et al. addresses the synthesis of semi-synthetic hydrogels by combining protein-based biomaterials, such as albumin, gelatin, and fibrinogen, with a synthetic polymer, poly(ethylene glycol) (PEG). These materials are used to investigate dorsal root ganglion (DRG) cell expansion in a controlled environment as well as cell-mediated 3-D invasion linked to peripheral nerve regeneration. The protein components imitate the extracellular matrix (ECM) to control neuronal cell morphogenesis, while the synthetic polymer creates a crosslinked network with regulated mechanical characteristics and degradation

[32].

As already mentioned, hydrogels can be engineered to mimic the extracellular environment of bodily tissues and they are suitable for drug delivery systems, for biosensors and for medical implants [25]. They are designed for medical applications due to their porous structure, biocompatibility, and biodegradability. They can swell and entrap therapeutic agents [Fig. 2.2], making them a potential drug delivery system [33].

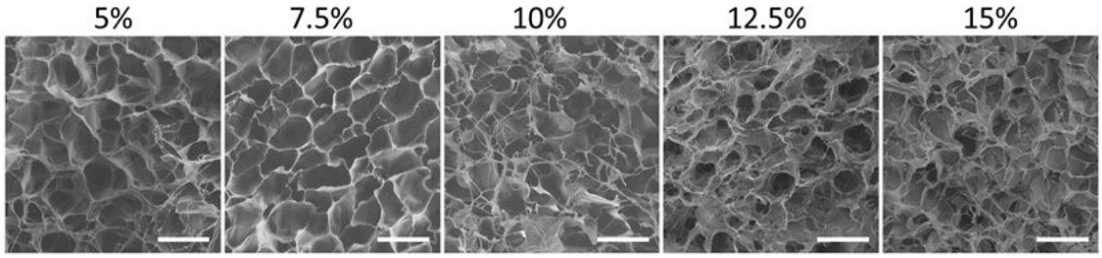

Figure 2.2: Swelling in a drug delivery hydrogel caused by a variety of chemical and physical processes. Yellow dots are the medication molecules and red and green lines are the matrix of the hydrogel [34].

Model hydrogel systems have led to significant discoveries in stem cell research, cancer biology, and cellular morphogenesis. Performance-based materials engineering continues to drive design advances in hydrogels' clinical applications [25]. In vivo studies show their effectiveness in curing various diseases [33]. When we talk about hydrogels, we should also discuss organogels, which are semi-solid systems made up of a liquid organic phase trapped within three-dimensional networks by chemical or physical bonding. Because of their shown special qualities, these materials are utilized in a variety of applications, including food processing, anti-icing, anti-fouling, drug delivery systems, and droplet manipulation. They are regarded as promising materials having a great deal of room for advancement and real-world use. The liquid phase distributed within the three-dimensional grid is the primary distinction between hydrogels and organogels [35].

- Hydrogels employ a water-based solvent as a continuous phase, whereas organogels use organic solvents.

- Because organic solvents have a greater boiling point than hydrogels, organogels are better suited for operating conditions at higher temperatures.

- The components of organogels may have variable hydrophobicity, giving the materials greater adaptability in their various applications.

- Organogels' low adhesion properties and hydrophobic polymeric reticles make them ideal for uses like anti-ice and anti-fouling [35].

Hydrogels can be classified according to the type of crosslinking used in their manufacture, which is usually divided into two categories: chemical crosslinking and physical crosslinking.

2.2 Physical crosslinking

Physical crosslinking of polymer chains relies on interactions such as hydrophobic forces or charge condensation to create gels under reversible environmental triggers such as pH, temperature, and ionic strength. Making sure the network can hold a significant amount of water and that there are strong inter-chain contacts for semi-permanent connections are important considerations when choosing polymers for gel formation. The gel's structure is supported by hydrophobic, electrostatic, and hydrogen bonding forces, making it reversible because these connections are purely physical [36] [37].

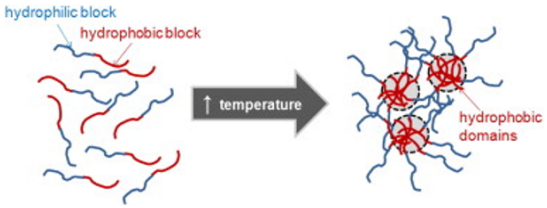

Figure 2.3: Hydrophobic interactions [37].

2.2.1 Hydrophobic interactions

Polymers with hydrophobic domains can produce gels in water using a technique known as reverse thermal gelation, or 'sol-gel' chemistry. These polymers, called gelators, have hydrophobic regions that drive mechanisms of cross-linking and they are moderately hydrophobic [Fig. 2.3]. Gelators are made by synthesizing block copolymers or by grafting a hydrophobic section on a hydrophilic polymer. At lower temperatures, these amphiphilic polymers dissolve in water; but, as the temperature rises, the hydrophobic segments group together to minimize their exposure to water. By reducing the hydrophobic surface area in contact with water, this aggregation lowers the amount of structured water surrounding these domains and raises the solvent's entropy. The gelation temperature is affected by the concentration of the polymer, the length of the hydrophobic block, and the chemical structure of the polymer; a lower gelation temperature is the result of more hydrophobic segments

since they increase the entropic cost of water structuring and significantly drive aggregation [37].

2.2.2 Electrostatic interactions

Charge interactions are intensively investigated for cross-linking, which has the advantage of promoting biodegradation because ionic species in extracellular fluid compete with gel components, resulting in network decross-linking. Furthermore, the cross-linking of microparticles or nanoparticle gels is made possible by this technique, which improves their applicability for drug delivery applications. Hydrogels can be formed by these interactions between two polymers of opposite charges or between a polymer and a tiny molecule [Fig. 2.4]. For example, in physiological settings, cationic lysine residues and anionic organophosphorus cross-linkers electrostatically interact to form cross-links in elastin-like polypeptides. Ionic-complementary peptides with alternating positive and negative charge domains that self-assemble into hydrogels in situ can be involved in polymer-polymer cross-linking. Another example is a combination of glycerophosphate and quaternized chitosan that, at physiological temperature, forms an ionically cross-linked gel and can release doxorubicin hydrochloride in a pH-dependent manner [36] [37].

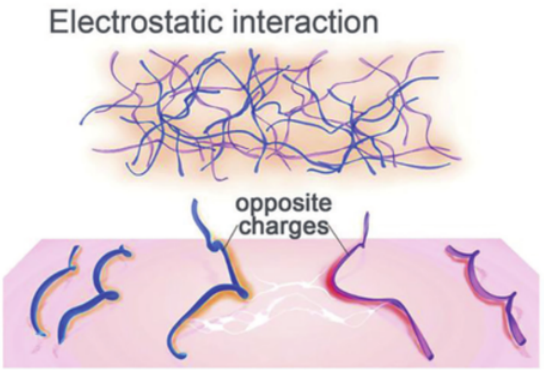

Figure 2.4: Electrostatic interactions [38].

These hydrogels, often referred to as in situ gelling hydrogels, can be created in situ and tailored for certain mechanical, thermal, and degrading properties. The ability of ionic/electrostatic interactions to self-heal, which permits the physical network of hydrogels to fracture under stress and rebuild following stress removal, is an extra advantage. Nevertheless, the cross-linking strategy's limitations limit their mechanical strength [39].

2.2.3 Crystallization

Crystallization is the process by which a solid forms where there are highly ordered atoms or molecules that repeat in all three spatial dimensions. A variety of scientific and industrial operations, such as the formation of crystals in nature, the synthesis of medications, and the development of materials with certain features in disciplines like chemistry, materials science, and geology, depend on crystallization. This technique uses hydrogels to build polymer chains that crystallize and physically connect them together. One popular technique for turning polyvinyl alcohol (PVA) into a hydrogel is to freeze and thaw the PVA's aqueous solution several times. Several variables, such as the PVA's molecular weight, the solution's concentration, the freezing temperature and time, and the quantity of freeze-thaw cycles used, affect the final hydrogel's characteristics [39]. The degree of crystallinity and crystallization play a crucial role in defining the polymer's ultimate properties. Melting or diluted fluids can also lead to crystallization. As the solvent evaporates in diluted solutions, crystallization takes place, resulting in the creation of single crystals with folded chains aligned in a certain pattern.
Nucleation and growth are the two phases of the crystallization process. The first stage, known as nucleation, is the formation of tiny crystal nuclei under supersaturated circumstances because of the solution's division into areas with various entropies. Nucleation can be affected by variables like temperature, ionic strength, volume, and contaminants. The second phase, known as phase of crystal development, ensues after nucleation. In this stage, the polymer chains align, and the nuclei grow, creating layers known as lamellae that are folded like chains. Spherulites are bigger, spherical formations that result from the aggregation of these lamellae. When these lamellae are placed in an orderly fashion, polymers exhibit crystalline phases; when they are structured irregularly, they exhibit amorphous phases. Polymers typically crystallize from their molten state into spherulitic structures, and the diameter of these structures is determined by a number of parameters, including the molecular structure of the polymer, the location of nucleation sites, and the pace of cooling [39] [40].

2.2.4 Hydrogen bonding

Although hydrogen bonds [Fig. 2.5] are not very strong on their own, they are an important part of hydrogel formation. These bonds have the ability to stabilize structures in hydrogel, especially in those made up of peptides or agarose. Hydrogels may have hydrogen bonds between groups such as starches, urea, carboxylic acids, and hydroxyl, or with electron donors such as pyridine and imidazole. Their collective interaction is powerful, even if typically a hydrogel is not supported by a single hydrogen bond [39].
Hydrogen bonding can be used to generate hydrogel through the use of freeze-thaw

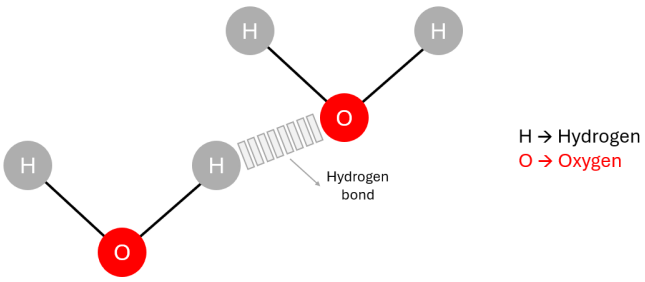

Figure 2.5: Hydrogen bond

and by creating injectable gels. When combined, natural polymers often exhibit rheological synergy, exhibiting viscoelastic qualities that are closer to gel than when each polymer is used alone. The creation of hydrogen bonds between suitable polymers is the cause of this effect. These connections form a physically crosslinked structure that is injectable and generally biocompatible, because they don't rely on chemical bonding. For instance, combinations like hyaluronic-methylcellulose acid cellulose, starch-carboxymethyl cellulose, and gelatine-agar result in physically crosslinked gels that are biocompatible, injectable and they resemble the body's extracellular matrix. However, these hydrogen-bound gels can't be utilized for very long because they disintegrate over time due to their water absorption [37]. In a study, You et al. developed a hydrogel with a mixture of strong and weak hydrogen bonds between N,N-dimetylacrylamide (DMAA), acrylic acid (AAc) and 2-ureido-4[H]-pyrimidinone units. They balanced the size of the monomers and their interactions to optimize the properties of the hydrogel [41]. Yoshimura et al. made a biodegradable hydrogel without a cross-linker. They esterified the starch with succinic anhydride, neutralized it and the product was dialyzed. The reformation of hydrogen bonds caused gelation during dialysis; this shows that hydrogen bonds can drive the process even in the absence of traditional cross-linkers [42].

2.2.5 Stereocomplexation

Interactions between polymeric chains or small molecules with the same chemical structure but distinct stereochemistry are referred to as "stereocomplexation". This method is essential for building strong structures without the need of chemical crosslinkers or harsh solvents [36]. Natural polymers can also utilize stereocomplexation for gelation. For example, dextran implanted with oligomers D- lactyl and L-lactyl can form gels in water spontaneously. Because they are extremely biocompatible and biodegradable, these gels are ideal for biomedical applications.

Stereocomplexation is an excellent choice for sensitive applications and environments because it does not require organic solvents or chemical interconnectors. On the contrary, the main obstacle is the narrow range of acceptable polymer compositions, as small changes to the stereochemical or polymeric structure can hinder or prevent the formation of complexes. This method can be used to create injectable gels or hydrogel with high storage moduli. These hydrogels have excellent mechanical properties and can be used for specific uses [36] [37].
Physically crosslinked hydrogels produce gels without the need of crosslinkers additions in vivo or chemical modifications. But they have some limitations. Since the strength of these hydrogel is strongly linked to the intrinsic chemical properties of the gel-forming agents, it is difficult to independently control variables such as freezing duration, pore size, chemical functionality and degradation rate. This limits the freedom of creation of these types of hydrogels. Furthermore, since these hydrogels dissolve and disperse over time, moreover, these hydrogels often have poor retention in the tissues because they dissolved and dissipate over time [37].
Conversely, the dilution of the hydrogel matrix and the diffusion of the polymer away from the injection site are prevented by covalent cross-linking, which produces more robust and stable gel formations.

2.3 Chemical crosslinking

Chemical crosslinked hydrogels have stronger and more permanent bonds than physically crosslinked hydrogels because they are formed through covalent bonds between polymeric chains. Generally, these hydrogels are more stable in physiological conditions. They also have better mechanical properties and controllable degradation rates [39].
Chemical hydrogels, also known as permanent hydrogels, often show regions with different densities of crosslinking. Areas with high crosslinking density and low swelling capacity, known as clusters, are found in areas with a lower density, and a higher swelling index. This non-uniformity results from the hydrophobic interaction of the crosslinking agents. Furthermore, phase separation and macropore formation within the gel structure can be caused by elements such as composition, type of solvent, temperature and solid concentration during freezing [40].

2.3.1 Photopolymerization

Photopolymerization is a versatile method for producing hydrogel networks with controlled properties. This makes them suitable for applications in tissue engineering, drug delivery and regenerative medicine. This technique uses photo-initiators that activate a chemical reaction when irradiated by UV light (200-400 nm) or visible light (400-800 nm), quickly forming a network of polymers that absorb

certain wavelengths of light [36] [39].
Because of their unique advantages, stimulus-responsive hydrogels, especially light-sensitive ones, have attracted scientific interest. Light stimuli are easy to control by switching on/off, they have a precise dosage adjustment, spatial and temporal control of biological processes and targeted application inside the optical tissue window. Light-responsive hydrogels are ideal for applications that require better control and modulation, such as 3D tissue engineering and controlled drug delivery. Poly (ethylene glycol) diacrylate (PEGDA), gelatin methacryloyl (GelMA) and methacrylated hyaluronic acid (MeHA) are some of the most common materials used to produce photopolymerized hydrogel. Due to their biocompatibility, hydrophilicity and ability to naturally degrade over time, these materials are ideal for biomedical applications [43].
Typically, a photosensitive system includes photo-initiators, pre-polymers, and potentially cells or therapeutic agents. In mild conditions, light energy causes the polymerization of pre-polymers. Free radical photopolymerization [Fig. 2.6], which is mainly used with pre-polymers functionalized with (met)acrylate, works through a chain growth mechanism. The free radicals produced by the photons absorbed by the photoinitiators react with the vinyl bonds in the pre-polymers, creating chemical bonds between the polymer chains. Hydrogel can be further modified using cellular adhesive components and replicable degradation sites [44].

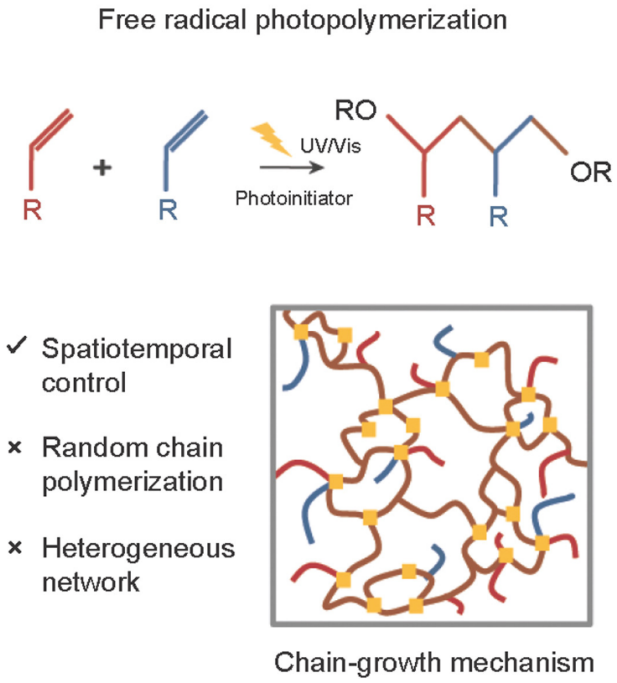

Figure 2.6: Free radical photopolymerization [44].

To ensure an ideal polymerization rate and minimize cytotoxic effects on embedded cells and surrounding tissues, it is crucial to choose an appropriate photo-initiator. Water solubility, stability, absorption spectrum, molar absorbability and efficiency in free radicals generation are important factors in choosing the photoinitiator. Photoinitiators are currently classified into two main categories: radical and cationic. Radical photo-initiators are preferred in biomedical applications because they are more biocompatible. Cationic photo-initiators, on the other hand, produce protonic acids, which makes them less useful in such applications [44]. In this specific thesis two photo-initiators were used, the LAP and the TPO.

1. LAP (Lithium phenyl-2,4,6-trimethylbenzoylphosphinate): is a radical photo-initiator [Fig. 2.7]. It has been synthesized and studied for its ability to initiate polymerization, in the photoencapsulation of living cells. LAP demonstrated high solubility in water, facilitated polymerization rates under light at wavelengths of 365 nm and had an absorption capacity extending beyond 400 nm, which allowed excellent polymerization of visible light. Systems initiated with LAP obtained cell survival rates of 95% or higher in all tested conditions when used to encapsulate fibroblasts in PEG diacrylate hydrogel [45].

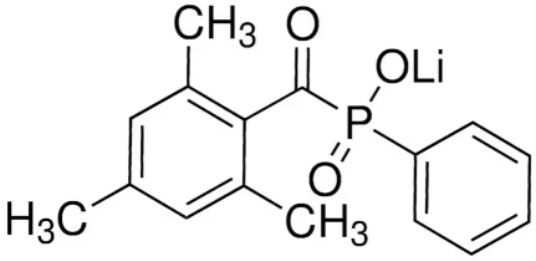

Figure 2.7: LAP chemical structure [46].

2. TPO (Diphenyl(2,4,6-trimethylbenzoyl)phosphine oxide): is a radical photo-initiator widely used in photo-polymerizable materials such as composite resins and dental adhesives [Fig. 2.8]. TPO mainly absorbs light in the ultraviolet range, with an absorption spectrum of 420-440 nm. It is effective under ultraviolet light sources with this range of wavelengths. TPO is known for its high curing efficiency that allows resin systems to polymerize quickly and have a high degree of conversion (DC). Finally the TPO can cause problems with the formulation, TPO requires formulation adjustments to increase its dispersibility in aquatic environments due to its low solubility in water. This complicates its use in hydrophilic or biomaterial adhesives [47].

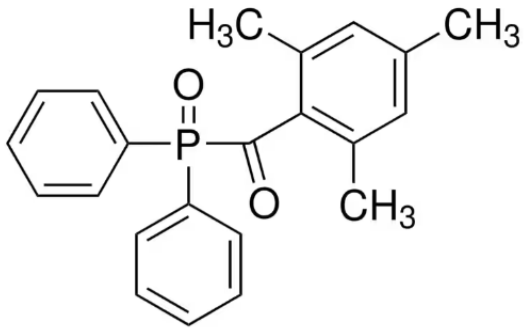

Figure 2.8: TPO chemical structure [48].

2.3.2 Enzymatic cross-linking

The process of forming hydrogel in situ through enzyme-catalyzed reactions is known as enzymatic cross-linking. This procedure uses specific enzymes to accelerate the formation of covalent bonds between polymer chains, which leads to the development of a crossed hydrogel network. For example, transglutaminases (TGs) are enzymes that catalyze the formation of covalent bonds between the free amino group of a protein or of a peptide-bound lysine and the γ-carboxamide group of the protein or peptide bound glutamine. Some of the advantages of this technique are:

1. Mild Conditions: Enzyme cross-linking does not require compounds like initiators, cross-linking agents or monomers, unlike conventional techniques. This eliminates the need of pre-functionalizing the polymer or irradiation.

2. High specificity: Enzymes often have a high degree of substrate specificity, which reduces side reactions and allows predictable and controlled interconnection kinetics.

3. Suitability for gelation in-situ: the gel is produced directly at the application site, such as in biological environments or in therapeutic applications.

The enzyme reacts with the substrates available in the polymer matrix, creating covalent bonds and creating an interconnected stable structure, as shown in Fig. 2.9. This method avoids complicated chemical processes and aligns well with biological systems, improving the compatibility and functionality of the hydrogel produced [36] [40].

2.3.3 Smart hydrogel

Smart hydrogels are sophisticated polymers with the ability to react to certain external stimuli, such as light, pH, temperature or chemicals. These stimuli-responsive

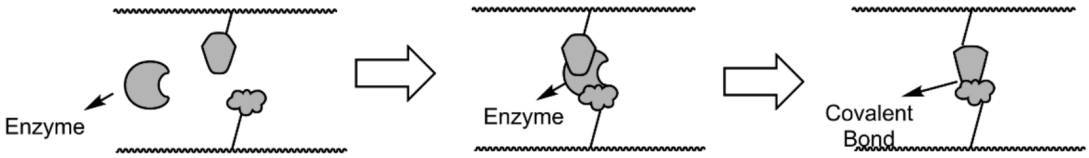

Figure 2.9: Enzymatic crosslinking method [40].

hydrogels can significantly alter their physical properties, such as increasing swelling or shrinkage. When activated, they can also release drugs or other agents. They are adaptable for drug delivery applications because of their dynamic activity, which allows the medication to be released in reaction to changes in the body, such as pH. Smart hydrogels not only transport medications but also serve as scaffolds in tissue engineering, where they may react to biological cues to help in tissue healing and cell proliferation. Furthermore, they are suitable for creating sensors that detect biomolecules, pH or temperature, thanks to their ability to adapt to environmental changes. They are used in contact lenses for sustained drug delivery to the eye. Smart hydrogels, which were first introduced in 1948, have developed into important tools in the medical and technological fields, providing effective and flexible solutions based on their ability to respond reversibly to external stimuli [39] [40].

2.4 Hydrogel strain sensors

Sensors can identify and measure electrical signals that are produced by physiological processes in humans, giving an indication of the body's health and offering cautionary advice. They are able to keep an eye on vital signs including blood pressure, respiration, and pulse, all of which are strongly linked to a number of illnesses. When sensors are incorporated into the human body, they must be pliable, stretchable, and have an elastic modulus that is comparable to the skin or tissue. Additionally, they must be able to detect mechanical deformations brought on by both tiny and big forces without moving away from the surface of the body. Sensors should also have a large detection range, high sensitivity, and be composed of biocompatible and biodegradable materials [14].
Hydrogel-based sensors are used for a variety of applications, such as soft robotics and human motion monitoring [49]. The capacity of these sensors to respond to external stimuli and transform chemical energy into mechanical energy makes them suitable for different applications [50].
For hydrogel-based sensors, there are several important parameters:

- Sensitivity or Gauge Factor (GF): is the sensor's ability to detect small changes

in the measured parameter, in particular is given by the formula:

$$GF = \frac{\Delta R/R_0}{\Delta l/l_0} = \frac{\Delta R/R_0}{\epsilon} \tag{2.1}$$

Where ΔR is the change in resistance due to deformation, R_0 is the undeformed initial resistance, Δl is the is the difference between the current length and the initial length; l_0 is the initial length and ϵ is the strain. This capability is critical for applications such as tracking small changes in human activity or physiological signals. Zhang et al. [51], for example, emphasizes how their hydrogel film-based sensor can precisely capture human motion signals and identify surface textures and roughness thanks to its 2.1-gauge factor and 200 ms reaction time (Fig. 2.10A). Applications in smart devices and human-machine interfaces require great sensitivity.

- Limit of detection (LOD): is the lowest strain that a sensor is capable of accurately identifying. This is especially relevant for health monitoring systems, because it might be very important to identify physiological issues early on. Xia et al. [49] developed a hydrogel-based strain sensor to identify both small and large-scale human activities, such as faint blood pulsations, emphasizes the significance of a low limit of detection for precise and timely health monitoring (Fig. 2.10B).

- Mechanical Properties: wearable sensors' comfort and longevity depend greatly on their toughness, flexibility, and elongation at break. For instance, Wu et al. [52] mention that their hydrogel films have a high break-over elongation of more than 900% (Fig. 2.10C).

- Self-Healing Capability: is the ability to mend itself after damage and this increases the longevity and durability of the sensor. Xia et al. [49] emphasizes that the hydrogel's capacity for self-healing is critical to sustaining sensor function over time.

- Biocompatibility: For sensors that come into contact with human skin or are used in medical applications, biocompatibility is essential to avoid adverse reactions [49].

- Adhesiveness: for wearable sensors, the ability to stick to different surfaces, including skin, is crucial. The hydrogels produced by Xia et al. exhibit a self-adhesive behavior on materials like polytetrafluoroethylene, wood, glass, aluminum, rubber, and skin [49].

- Stability: the stability of the sensor under a range of environmental conditions, including change in temperature, is essential to its long-term functioning. Wu

et al. show their organohydrogels with improved freezing and drying tolerances over ordinary hydrogels [52].

- Response Time: For real-time monitoring applications, the sensor's response time to changes is crucial. As already mentioned before, Zhang et al. [51] report a response time of 200 ms for their hydrogel film-based sensor, which is suitable for real-time applications.
- Multistimuli Sensitivity: sensors that can react to a wide range of environmental stimuli, including temperature, humidity, and gas, can have a wider range of applications. Wu et al. highlights how sensitive their hydrogel-based sensors are to a variety of stimuli, including strain, temperature, humidity, and gas [52].

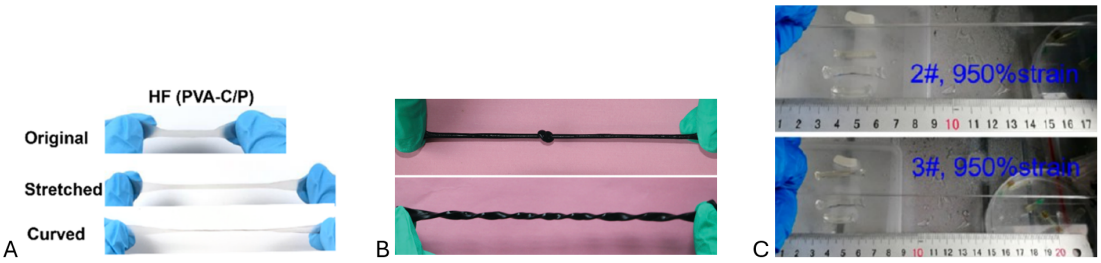

Figure 2.10: Mechanical properties of different hydrogels. A) Hydrogel prepared by Zhang et al. [51], B) Hydrogel prepared by Xia et al. [49], C) Hydrogel prepared by Wu et al. [52].

2.4.1 Piezoresistive sensor

A piezoresistive sensor (Fig. 2.11) measures the change in electrical resistance that occur when a material is deformed, in order to detect changes in strain. These sensors can be combined with hydrogels that are sensitive to analytes to create biochemical sensors that can track a variety of chemical and biological events. The fundamental idea, referred to as the piezoresistive effect, is that changes in the material's resistance as a result of structural deformation translate into changes in electric current. The resulting electrical signals provide a direct representation of the magnitude and frequency of the applied force, with sensitivity often quantified by the gauge factor (GF) [20] [53].
As studied by Schmidt et al. analyte-specific hydrogels, such as those derived from hydroxypropyl methacrylate (HPMA), 2-(dimethylamino)ethyl methacrylate (DMAEMA), tetraethylene glycol dimethacrylate (TEGDMA), and ethylene glycol (EG), are frequently integrated with microfabricated pressure transducers in

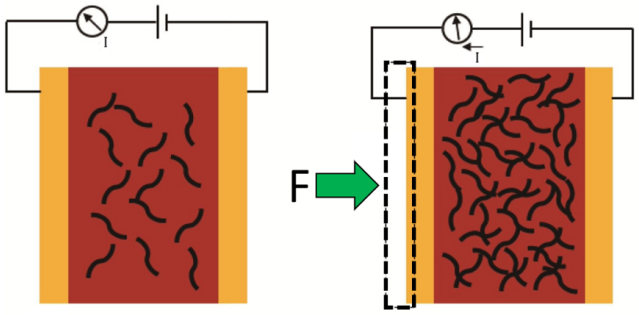

Figure 2.11: Change in electrical resistance of a piezoresistive sensor that occur when a material is distorted (picture modified by [54]).

piezoresistive sensors. After being polymerized to maximize their sensitivity and swelling, these hydrogels are used in implantable sensors with parylene C coatings and dip sensors, among other designs [53]. The sensors are usually made of flexible substrates (such polyimide, PDMS, and Ecoflex) paired with conductive fillers (metals or semiconductors like graphene and carbon nanotubes).
Many sensors on the market require wired connections to monitoring systems, which can be difficult to use and can cause restrict mobility. Therefore, even if it's still in its early stages, the development of wireless and remote monitoring capabilities is a promising direction for next-generation intelligent sensors. With its remarkable thermal and electrical characteristics, graphene exhibits a lot of promise in this rapidly developing field [20].
Piezoresistive sensors are widely used for continuous monitoring of metabolites, pH, and glucose levels in physiological solutions. Their applications extend prominently into biotechnology and medical fields, where they offer several advantages such as cost-effectiveness, robustness, miniaturization, and in-line capability, so they can be integrated directly into systems for real-time analysis. These characteristics make piezoresistive sensors ideal for applications in continuous glucose monitoring, bioprocess monitoring, and clinical diagnostics [53] [55].

2.4.2 Capacitive sensors

Compared to resistive sensors, capacitive sensors (Fig. 2.12) provide a number of advantages, including better linearity, increased thermal stability, and less hysteresis. These sensors usually work with a parallel-plate arrangement, in which two electrodes are separated by a dielectric layer. Variations in the separation between these plates alter the capacitance. The dielectric layer becomes thinner when external pressure is applied, which increases capacitance. By monitoring these variations in capacitance, capacitive sensors are able to detect a wide range

of physical phenomena, such as touch, pressure, strain, and proximity. The basic design consists of conductive materials divided by a dielectric layer, and changes in the dielectric's characteristics or distance from each other impact the measured capacitance [14] [56].

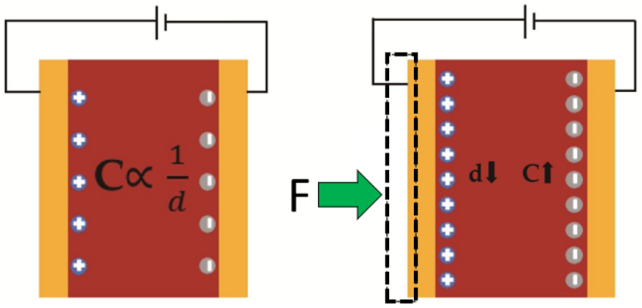

Figure 2.12: Change in capacitance of a capacitive sensor that occur when a pressure is applied (picture modified by [54]).

The capacitance value is determined using the equation:

$$C = \frac{\epsilon A}{d} \tag{2.2}$$

Where ϵ is the dielectric constant, A is the plate area, and d is the distance between the two parallel plates. As with the resistive-type sensors previously mentioned, a capacitive sensor's sensitivity can be described as follows:

$$S = \frac{\Delta C/C_0}{P} \tag{2.3}$$

Where ΔC is the change in capacitance, C_0 is the initial capacitance, and P is the pressure applied.
Various materials and unique structures can be used to create capacitive sensors. Mo et al. [56], for example, describes a dynamically super-tough hydro/organogel-based capacitive strain sensor. This sensor achieves excellent linear sensitivity and good stretchability by using an organogel dielectric in conjunction with dual-crosslinked hydrogel conductors. Its construction makes it resistant to severe mechanical stress, such being run over by a car, and it can track a variety of human actions in addition to tiny physiological indications. Similarly, Kweon et al. [57] describes a hybrid hydrogel-based multimodal capacitive sensor that includes poly(vinyl alcohol) (PVA), sodium tetraborate decahydrate, poly(N-isopropylacrylamide) (PNIPAAm), and poly(sodium acrylate) (SA). This sensor can detects touch and temperature simultaneously and it responds in 0.3 seconds. In Chen et al. work [58], is described a wearable hydrogel sensor with an affordable ionic-digital converter. It

uses transparent, biocompatible ionic hydrogels for pressure and gesture recognition, and it stays functional even after extended exposure to air.
Capacitive sensors are used in robotics, wearable biomedical devices, human-machine interfaces, and smart windows. They are used to measure touch pressures, recognize gestures, monitor physiological signals, and sense temperature changes.

2.4.3 Piezoelectric sensors

The piezoelectric effect's reversibility allows mechanical or vibrational energy to be converted into electrical energy and vice versa. Materials with piezoelectric characteristics include inorganic ceramics and organic polymers. This effect is used by a piezoelectric sensor (Fig. 2.13) to convert mechanical stress into electrical impulses. Some materials develop an electric charge when mechanical tension is applied, which allows the sensor to produce electrical energy from mechanical input. Piezoelectric sensors can be crafted from a variety of materials using different fabrication techniques [14].

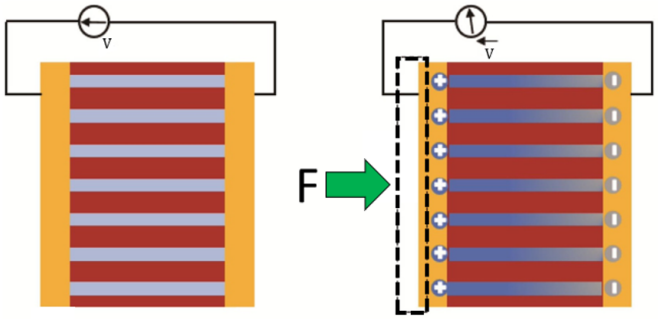

Figure 2.13: Change in electrical impulse of a piezoelectric sensor that occur when a deformation is applied (picture modified by [54]).

Piezoelectric sensors are widely used, especially in wearable technologies and the biomedical industry. According to Du et al. [59] these sensors are employed in wound healing, energy harvesting, bio-signal detecting, and ultrasonic stimulation. Fan et al. [60] say that hydrogel-based piezoelectric materials (H-PEMs) are employed in smart wearables to track motions of body parts such the wrists, ankles, feet, and fingers. Additionally, they find employment in implantable medical devices that are employed in the skin, heart, and bones.

2.4.4 Triboelectric sensors

Static electricity is produced via the triboelectric effect, which happens when two materials come into contact, separate, and then exchange electrons. Triboelectric sensors, which use the friction between various materials to transform mechanical energy into electrical energy, can be made using this natural phenomenon. It is possible to use this phenomenon for energy collecting.
Triboelectric sensors use this phenomenon in sensing applications. These sensors can be crafted from various materials that differ in triboelectric polarity. Combining materials with opposing triboelectric charges and creating structures that optimize their contact area are key to maximizing their effectiveness. Traditional sensors often rely on mechanical fixtures, which can be uncomfortable. Triboelectric sensors, on the other hand, may be easily included into flexible fabrics to improve user comfort, eliminating the need for mechanical fixtures. For example, an all-textile triboelectric sensor (ATTS) was fabricated by integrating conductive sensing yarns, made from stainless steel and polyester fibres, into commercial garments. This approach not only captures human gestures but also ensures a compact and optimized contact area, improving the sensor's electrical output.
Triboelectric sensors are convenient because they can be easily incorporated into common materials like textiles. This allows wearable electronics to be used without the disadvantages of conventional sensors, such pain or the possibility of skin irritation from adhesives. These sensors are also extremely ideal for practical usage since they can be made on an industrial scale while maintaining great sensitivity, stability, and washability. Triboelectric all-textile sensor arrays (TATSAs), for instance, exhibit these qualities by efficiently monitoring arterial and respiratory pulse signals and being machine-washable and stable over prolonged use [14].

2.4.5 Ionic-conductive hydrogel sensors

An ionic-conductive effect involves the movement of ions, which are electrically charged particles, within a hydrogel matrix, which provides the material with its conductivity. In an ionic-conductive sensor, mechanical deformations such as strain, pressure, and motion are detected by measuring changes in electrical resistance or capacitance. These changes occur due to alterations in the ionic pathways to the electrodes caused by the sensor's deformation. These sensors are typically fabricated from hydrogels containing specific ionic networks that allow ions like Fe^{3+}, SO_4^{2-}, or Li^+ to move freely, enabling the detection of mechanical changes [61] [62].
The fabrication process can vary, such as the use of dual ionic networks formed through polymerization and soaking [61], or the creation of zwitterionic composite hydrogels from waterborne polyurethanes and poly(sulfobetaine zwitterion-co-acrylamide) [63], which enhances both mechanical strength and ionic conductivity.

Yang et al. describes a rapid fabrication method for a hydrogel using agar and polyacrylamide (PAM). Agar creates a physically cross-linked network, complemented by PAM which forms a photoinitiated cross-linked network under UV light exposure. This dual-network structure incorporates Li+ ions to impart ionic conductivity. The hydrogel produced through this process is versatile and can be molded into different shapes using injection molding techniques [62].
Ions are able to move through the porous networks in ionic-conductive hydrogels. The hydrogel's conductivity is determined by the ion concentration.
In solutions with low concentrations of electrolytes (such as salts dissolved in water), the total number of ions present (both positive and negative ions) is relatively low. In these low-concentration solutions, the overall conductivity (the ability to conduct electricity) is primarily influenced by the total number of ions dissolved in the solution. This means that the more ions there are in the solution, the better it can conduct electricity. The concentration of ions directly affects the number of charge carriers available to carry current [64].
In contrast, high-salt solutions contain a much higher concentration of dissolved ions. This could be due to a higher concentration of the same electrolyte or a mixture of different electrolytes. In high-salt solutions, where the concentration of total ions is already high, the key factor influencing conductivity shifts from the total ion concentration to the mobility of the ions. This refers to how easily ions can move through the solution under the influence of an electric field. Higher ion mobility means ions can move more freely and thus contribute more effectively to electrical conductivity. Therefore, in high-salt solutions, the conductivity is largely governed by how fast the ions can move rather than how many ions are present (which is already high) [64].

Chapter 3

Materials and methods

3.1 GelMA-based hydrogel synthesis

3.1.1 GelMA synthesis

In this study has been synthesized gelatin methacryloyl (GelMA) with a procedure previously used by Vigata et al. [65] and subsequently modified to perform the gelatin metacrylation reaction (Fig. 3.1).

1. 40g of cold-water fish gelatin, corresponding to 20% by weight, provided by Sigma-Aldrich (Darmstadt, Germany), was dissolved in 200 mL of distilled water with a neutral pH at room temperature (RT) using a magnetic stirrer (AREX-6 Magnetic Hot Plate Stirrer sold by Velp Scientifica).

2. Once solubilized, i.e. when the solution becomes clear after roughly 40 minutes, the pH was adjusted at 9 with a solution of sodium hydroxide 3M (NaOH), prepared by dissolving 12g of NaOH provided by Sigma-Aldrich in 100 ml of distilled water.

3. A ratio of 1:0.6 between gelatin and methacrylic anhydride (MA) also provided by Sigma-Aldrich, corresponding to 12g of methacrylic anhydride, was added dropwise to the previous solution. The MA was added dropwise to ensure a uniform mixing of the solution. During this process, the reaction was maintained at a constant temperature of 40°C under continuous stirring for a total period of 4 hours. In the first 2 hours, the pH of the solution was adjusted to 9 every 15-20 minutes to ensure optimal reaction conditions. Subsequently, for the remaining 2 hours, the pH was monitored and adjusted every 30-40 minutes. This periodic pH control was crucial because a higher pH increases the reactivity of amine and hydroxyl groups, promoting a higher degree of

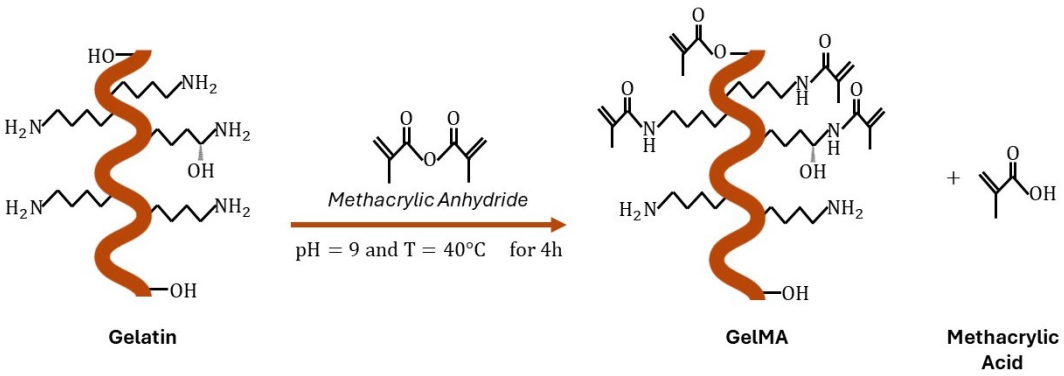

Figure 3.1: Scheme of the reactions for the synthesis of GelMA.

substitution and enhancing the effectiveness of the chemical modification. The experimental setup used is shown in Fig. 3.2.

Figure 3.2: Experimental setup used for GelMA synthesis.

4. Once finished the solution was dropped into membranes with a molecular weight cut-off (MWCO) of 12-14 kDa, used for the dialysis process. This size of the pores enables the separation of gelatin that has reacted with MA from unreacted gelatin and excess MA. The pores of the dialysis membrane are sufficiently large to allow the passage of methacrylic anhydride (MA) and the amino acid chains that make up gelatin, which can leak out of the membrane, while retaining the larger GelMA molecules due to their greater molecular size. The filter bags were dialyzed for five days at neutral pH in a laboratory glass beaker using distilled water on a magnetic stirrer at 200 rpm. The dialysis liquid was changed twice daily for the first two days and once daily for the remaining three days. Process and experimental setup showed in Fig. 3.3.

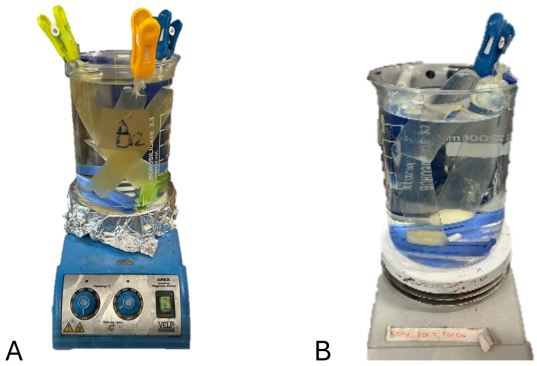

Figure 3.3: Dialysis of GelMA. A) On day 0, the solution inside the dialysis membrane appears yellowish and homogeneous. B) On day 5, the solution is significantly clearer, and phase separation has occurred.

5. At the end, half of the mixture was lyophilized using a 5Pascal freeze dryer (model LIO-5PDGT) at -40°C and under a pressure of about 0.5 Pa for approximately one week. The resulting product appeared as a whitish sponge, and it was stored at RT (Fig. 3.4A). The other half of the solution was oven-dried for 48 hours at 60°C in glass Petri dishes lined with parchment paper. The dried product was then scraped off the parchment paper and ground with a laboratory mortar (Fig. 3.4B). This product was also stored at room temperature (RT).

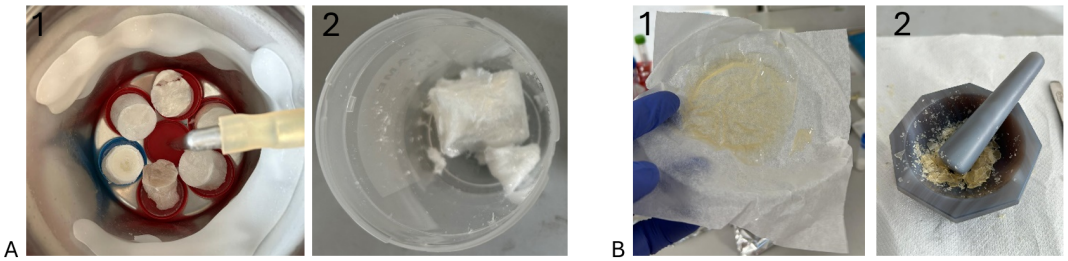

Figure 3.4: Preparation of lyophilized GelMA and desiccated GelMA. A) Freeze-drying of GelMA using the LIO-5PDGT freeze dryer (1) and the final product (2). B) Desiccation process where GelMA is first desiccated in the oven (1) and then ground with a laboratory mortar (2).

3.1.2 Hydrogel synthesis

Following the synthesis of the base material for sensor development, our focus shifts to preparing a hydrogel that exhibits the required conductive properties. The

development process will include optimizing the hydrogel's formulation to achieve the necessary conductivity, stability, sensitivity, and durability for its intended application environment.
The primary aim of this thesis was to investigate the removal of the aqueous component from a GelMA-based hydrogel and replace it with a solvent that preserve biocompatibility. This approach seeks to enhance the sensor's stability and durability by eliminating the issue of water evaporation, which is a common problem in hydrogels that are intended for extended use. By addressing this problem, the goal is to potentially extend the sensor's operational lifespan.
To solve this issue, glycerol has been selected as the material. Glycerol is a viscous and transparent organic molecule with the chemical formula $C_3H_8O_3$, well-known for its high-water solubility. It is a triol, with three hydroxyl (-OH) groups, and is widely utilized in many different sectors because of its strong cytocompatibility and low toxicity.
However, the presence of glycerol alone makes it impossible to solubilize GelMA due to its chemical properties and the specific interactions required. Despite being a polar solvent, glycerol cannot establish the necessary interactions with the methacrylic groups and other functional groups of GelMA to promote solubility. Consequently, the addition of water was necessary to facilitate gelatin solubilization. Initially, it was important to determine the maximum concentration of GelMA that can be solubilized in water. A heated magnetic stirrer was used (carefully maintaining temperatures below 60°C to prevent gelatin chain denaturation) with a water bath set at 40°C. A vial containing a predetermined amount of water and a magnetic stir bar aiding gelatin solubilization was placed in the bath (Fig. 3.5).

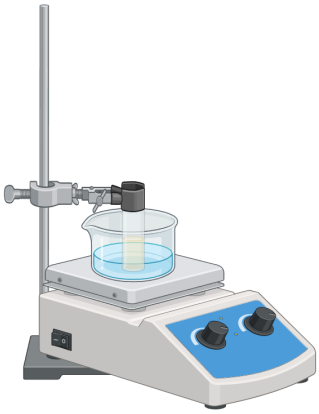

Figure 3.5: Experimental setup used for GelMA-based hydrogel synthesis.

GelMA was added incrementally in 10% w/v steps relative to the initial water volume in the vial. Excellent solubilization was achieved up to 80% w/v, beyond which the solution became highly viscous, slowing the process. Consequently, the

temperature was raised to 50°C to complete solubilization up to 100% w/v, resulting in a highly viscous yet uniform solution. Considering that additional agents will be added to the solution in the final formulation to enhance the electrical and mechanical characteristics of the sensor, it was decided to halt at this concentration, optimal for the intended application (Fig. 3.6).

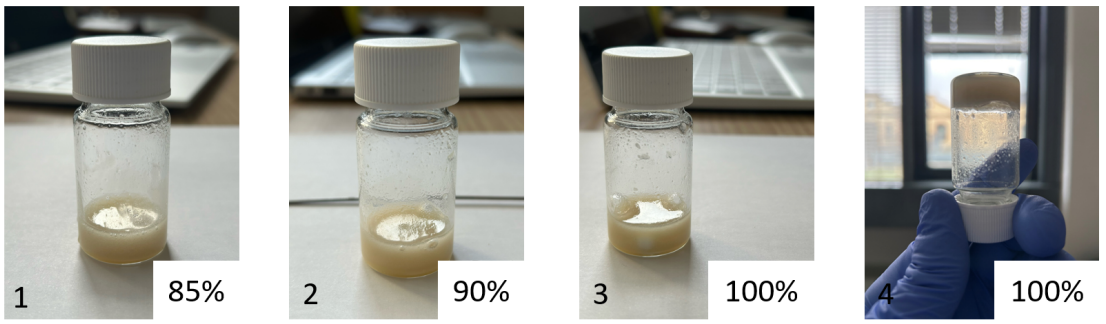

Figure 3.6: GelMA-in-water solubilization process (1-3) and viscosity of the 100% w/v solution (4)

With the intention of incorporating glycerol, further experiments were conducted to determine the appropriate concentration for this formulation. Starting with the 100% w/v formulation, the tested proportions were:

- 1:1 (one part water to one part glycerol), resulting in a GelMA concentration of approximately 50% w/v. This yielded a highly viscous solution that necessitated a spatula to be collected due to impracticality for pipetting, with the formation of numerous bubbles.
- 1:2 (one part water to two parts glycerol), resulting in a GelMA concentration of about 33% w/v, remained too viscous and unsuitable for pipetting.
- 1:4 (one part water to four parts glycerol), resulting in a GelMA concentration of 20% w/v, can be pipetted reasonably well with an acceptable level of bubble formation.

Given the objective of maximizing glycerol presence in the solution and considering that GelMA-based sensors typically exhibit concentrations of 15-20% w/v in water according to literature, the 1:4 ratio was selected for the subsequent steps. The next step is to enhance the electrical properties of the sensor by designing an ion-conducting device. Pure sodium chloride (NaCl) was chosen as the electrolyte

due to its accessibility, cost-effectiveness, and biocompatibility. Subsequently, a solution comprising water, glycerol, and salt was prepared. Since solubilizing salt in glycerol is difficult, it was decided to base the percentage of NaCl to be added solely on the amount of water present. The maximum theoretical molar concentration of NaCl in water at room temperature is 6.16 mol/L. Assuming a solution consisting of 5 parts in total, with only one part designated for salt dissolution, the achievable maximum concentration is therefore 1.232 mol/L. Considering a margin of error, a final concentration of 1 mol/L was chosen. A preliminary formulation was thus prepared for future experiments, comprising 20% w/v GelMA, equivalent to 20 mg of GelMA per 1 ml of solution. The solution was composed of a ratio of one part water to four parts glycerol (1:4) and had a NaCl concentration of 1 M. Subsequently, TPO (Triphenylphosphine oxide), a photoinitiator that generates free radicals upon exposure to UV light, was introduced into the formulation. These radicals initiate polymerization, aiding in the formation of chemical bonds between monomer molecules and thereby promoting the creation of polymer networks. According to literature, the minimum effective amount of TPO required to crosslink GelMA solution is 2% by weight of GelMA. The mixture is vacuum-sealed in a heated oven to eliminate air bubbles, with the solution kept at 50-55 °C to minimize viscosity (Fig. 3.7A). Next, the formulation is poured into dog bone-shaped PDMS mold (Fig. 3.7B), ensuring careful avoidance of bubble formation.

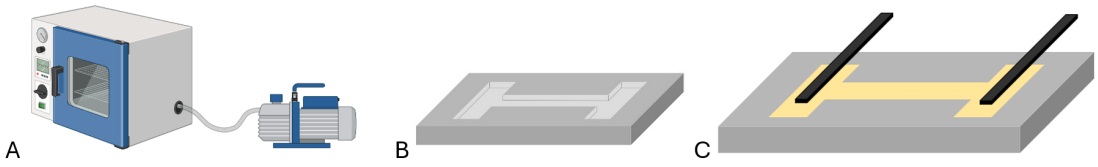

Figure 3.7: A) Scheme of experimental setup used for removing bubbles from GelMA solution. B) The dog bone-shaped PDMS mold. C) Position of the steel L360 electrodes.

PDMS, or Polydimethylsiloxane, is a transparent and flexible silicone used for its biocompatibility and optical properties. The preparation of a PDMS mold involves several key steps. Firstly, a master model is created in PMMA. Next, PDMS copolymer and the thermal curing agent are mixed in a ratio of 10:1 (10g of PDMS and 1g of thermal curing agent) and degassed to remove air bubbles. When the copolymer and curing agent are mixed, the crosslinking process begins, which can be accelerated by applying heat. So, the PDMS mixture is poured on the PMMA model, and it is placed in an oven at 60°C for a period of 24 hours. This heat treatment activates the cross-linking process, where the curing agent facilitates the formation of chemical bonds between the PDMS polymer chains. After curing, the PDMS mold is carefully peeled off the master mold.

The dog bone-shaped mold containing the formulation is placed under a UV lamp (Oriel Instruments model 97434-1000-1) emitting approximately 36 mW/cm^2 for 2 minutes to initiate crosslinking (Fig. 3.8). Afterward, the sample is carefully detached from the mold and turned upside down. Steel L360 electrodes are placed at each end (as shown in Fig. 3.7C), and additional formulation is poured on to secure them in position. Subsequently, the sample undergoes another 2-minute UV exposure.

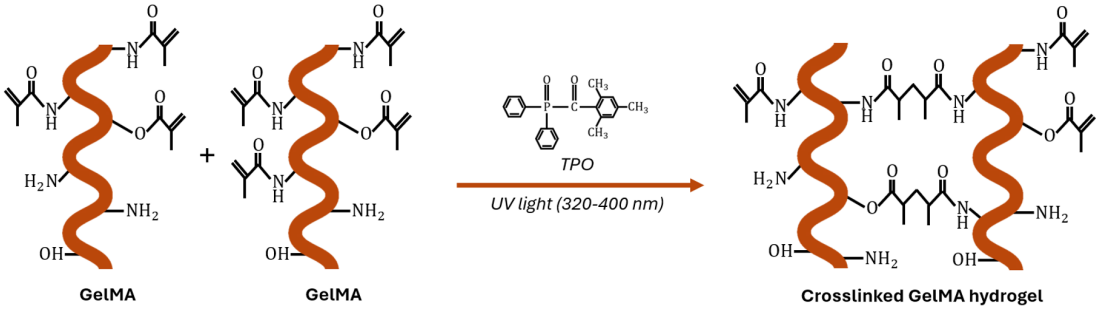

Figure 3.8: Scheme of the reactions for the crosslinking of GelMA.

After that, the sensor was ready to be tested.

3.2 Material characterization

3.2.1 Degree of methacrylation using formaldehyde (DOF)

The degree of methacrylation using formaldehyde (DOF) is a method used to determine the degree of methacrylation of GelMA. The term "methacrylation" refers to the presence of methacrylate groups in the polymer. The percentage of methacrylate functional groups in relation to all the functional groups in the material is expressed as a DOF. This measurement is important because it affects the properties of the gel, such as its reactivity, its cross-linking capacity and its mechanical characteristics. To perform the test, it was important to carefully follow these steps:

1. It is essential to heat the formaldehyde reagent solution, which contains OPA (o-phthalaldehyde), to room temperature in a Falcon tube. This step is crucial because OPA enables fluorescence detection and quantification by reacting with the primary amines of proteins, peptides, and amino acids. For this step is necessary to wait at least 3 hours. Alternatively, preparing a smaller Falcon tube can help speed up the process.

2. Prepare some gelatin solutions in PBS to establish the calibration standard curve, using the concentrations of 0 mg/mL, 0.02 mg/mL, 0.1 mg/mL, 0.5 mg/mL, 0.75 mg/mL, and 1.0 mg/mL. For best results use the same gelatin used to synthesize GelMA.

3. Prepare a GelMA solution in PBS using the concentrations of 1 mg/mL.

4. Heat all the solutions to 50°C and mix them until they are homogeneous and transparent. Then cool the solution to room temperature.

5. Prepare five (2mL)-Eppendorf microtubes with 300 µL of gelatin, one with 300 µL of GelMA solution and one with 300 µL of PBS solution (0 mg/mL gelatin) as shown in Fig. 3.9.

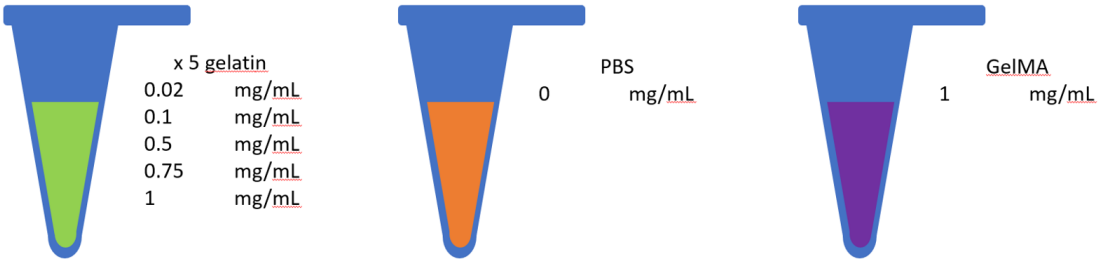

Figure 3.9: Preparation of the (2mL)-Eppendorf microtubes.

6. Heat the lamp of the fluorescence detector for at least 3 minutes before use.

7. Start a 5-minute timer. Mix each solution (the 7 Eppendorf tubes) with 600 µL of OPA. Pipette up and down in each microtube to mix the solution. Gelatin solutions of different concentrations can be mixed using the same pipette tip; however, use a new tip for the GelMA solution. Pipette 250 µL of each solution into three wells of a laboratory plate as shown in Fig. 3.10.

8. After 5 minutes, place the plate into the fluorescence detector to measure fluorescence at 450 nm using an excitation wavelength in the range of 460-360 nm (in this case 360 nm). Use the "Gen5 3.05" software for this procedure. The results will be displayed as numerical values, where N indicates fluorescence intensity: higher numbers correspond to stronger fluorescence and a darker background (Fig. 3.11).

Afterwards, extract the data provided by the software and input it into Excel to generate the calibration curve. Specifically, the degree of fluorescence (DoF) is calculated as:

$$DoF(\%) = \frac{C - X}{C} * 100 \tag{3.1}$$

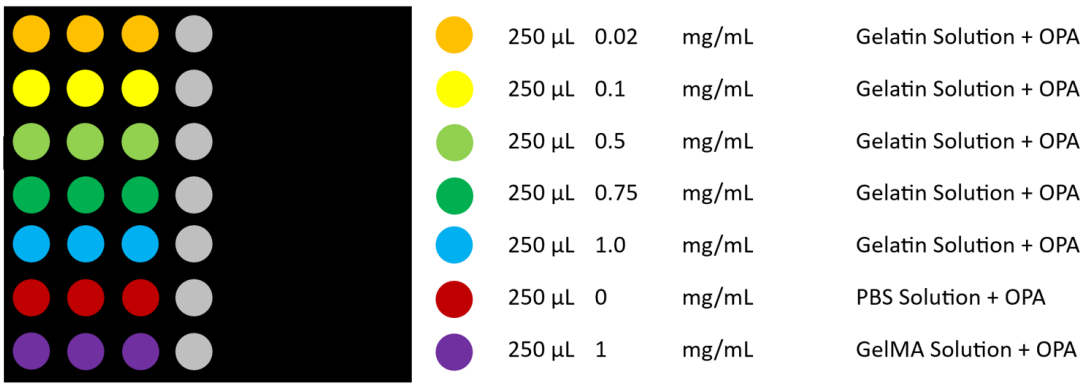

Figure 3.10: Preparation of the laboratory plate.

N	N	N
N	N	N
N	N	N
N	N	N
N	N	N
N	N	N
N	N	N

Figure 3.11: Example illustrating how the results are displayed in the software.

Where C represents the concentration of the GelMA sample and X represents the concentration of gelatin expressed in mg/mL.

3.2.2 Citocompatibility test

Cytocompatibility tests are important evaluations used to determine how well a material interacts with living cells. They're important in fields where it's crucial to comprehend how materials interact with biological systems and guarantee their efficacy and safety. They offer crucial knowledge for creating biologically compatible and naturally integrating biomedical sensors, drug delivery devices, and tissue scaffolds. The cytocompatibility test used HaCaT (human keratinocytes) cells, which reside on the outer layer of epithelial tissue, the selection of these cells is crucial for a strain sensor intended to be positioned on the skin. There are several types of cytocompatibility tests but in this work it was used the Cell Viability Assays method with MTT assay. The MTT assay, or 3-(4,5-dimethylthiazol-2-yl)-2,5-diphenyltetrazolium bromide assay, is a yellow tetrazolium salt that is reduced by living cells to formazan, a purple/blue-colored product, specifically within the mitochondria of viable cells. This reduction process is an indicator of metabolic activity, making the MTT assay a metabolic assay. The samples underwent ethanol

(EtOH) 70% washes to eliminate unreacted components, followed by PBS washes to remove residual ethanol. Following these washes, the samples were sterilized by exposure to two cycles of UV light for 30 minutes to eliminate other harmful substances. Subsequently, the samples were incubated in 10 ml of culture medium (DMEM + GlutaMAX-I) for 2 days to produce conditioned medium for use in the MTT assay.
The samples were covered with DMEM 1× (Gibco) supplemented with 10% FBS (fetal bovine serum, Thermo Scientific) and antibiotics 100 U/mL penicillin and 100μgmL streptomycin sulfate (Sigma-Aldrich). After 72h of contact between the culture medium and the samples at 37 °C, the media containing were collected (see images in next slide, the yellow color represents the acidification of the media). The media of every condition was then used to seed human keratinocyte (HaCaT) cells at a density of $1 * 10^4$ cells/well in a 96 well plate. After one and three days Live/dead and MTT assays were performed to assess cell viability. Cells were also seeded and analyzed in a PS well using DMEM 1x as an additional control.
The Live and Dead assay was used to test cell viability (LIVE/DEAD Viability/Cytotoxicity Kit, Sigma Aldrich). The test is based on the simultaneous determination of live (green) and dead (red) cells with two specific probes, calcein AM and Propidum Iodide (PI), respectively. After one ans three days of culture, cells were washed with PBS, stained with 1.5 μM Propidium Iodide (PI) and 1 μM Calcein-AM for 30 min in an incubator at 37 °C and washed again with PBS to remove the unreacted dyes. The fluorescence signals were detected using an Eclipse Ti2 Nikon (Tokyo, Japan) microscope equipped with a Crest X-Light spinning disk.
For the MTT assay is used the MTT. MTT is a reagent that function as a cell health indicator by using the cellular redox potential of live cells to quantitively measure Well viability and proliferation. MTT (0,5 mg/ml) was added to each well and then incubated at 37 °C for 2 h. The liquid in each well was tripped out and 200 μl DMSO was added to each well to suspend the cell layer. The above suspension was evaluated with a dual-wavelength spectrophotometer with the measurement wavelength at 570 nm and reference wavelength at 650 nm.

3.3 Hydrogel and sensor characterization

3.3.1 % Gel

The “percent gel” technique (Fig. 3.12) is a method used to evaluate the degree of crosslinking in polymeric materials. This technique measures the proportion of the polymer network that is crosslinked versus the portion that remains soluble.
The “percent gel” method is based on the principle that a fully crosslinked polymer forms an insoluble network (gel) that does not dissolve in solvents, while unreacted

or partially reacted polymers remain soluble.
A sample of the polymer is prepared through cross linking, and its initial weight (w_0) is measured. Then it is immersed in a solvent (in this case chloroform), and enclosed in a net to prevent any detached pieces from drifting away, for a 24h-period to extract the non-crosslinked components from the sample, causing them to dissolve into the solution. Afterwards, the sample is dried to remove any remaining solvent for 1 day and the final weight (w_f) is measured. For more precise measurement, initially, the weight of the net surrounding the sample was recorded. Subsequently, after treatment, the sample was weighed with the mesh, and then the weight of the mesh was subtracted to obtain only the weight of the sample. This weight was then compared to its initial weight.
The percent gel is calculated using the formula:

$$\%Gel = \frac{w_f}{w_0} * 100 \tag{3.2}$$

A higher percentage suggests a higher level of crosslinking, which means that a larger percentage of the polymer has created an insoluble network. Conversely, a lower percentage gel denotes less crosslinking and a larger amount of unreacted polymer that is still present.

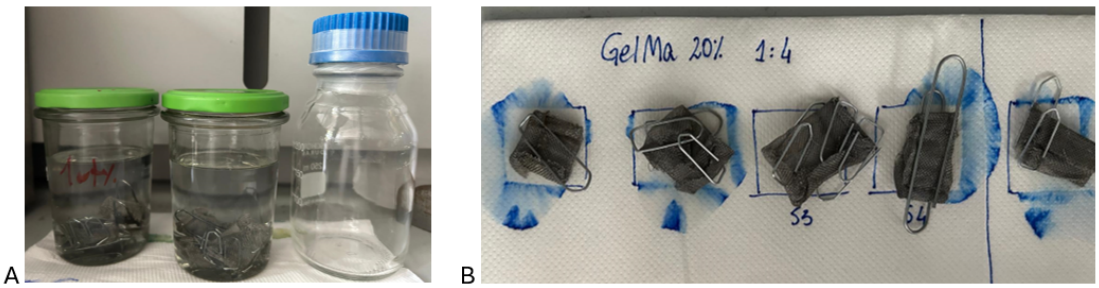

Figure 3.12: %Gel method. A) Hydrogel in chloroform and B) Drying process of samples.

3.3.2 FTIR-ATR spectroscopy

FTIR-ATR spectroscopy stands for Fourier Transform Infrared Attenuated Total Reflection spectroscopy. It is a method that evaluates how a sample absorbs infrared light within the mid-infrared spectrum, specifically from $4000cm^{-1}$ to $500cm^{-1}$. By merging the techniques of FTIR and ATR, this approach offers comprehensive insights into the molecular structure and composition of diverse materials.
At each specific wavelength, different types of chemical bonds show distinct thermal movements like bending, stretching, or torsion. By analyzing the spectrum obtained

from the instrument, it is possible to identify the components present in the material. After acquiring the signal, a Fourier transform process converts raw data into a spectrum, composed by multiple peaks where every peak reflects changes in a specific molecule's dipole moment. Notably, when working in absorbance mode, the amplitude of the peaks can also provide a quantitative estimation by comparing them.
The attenuated total reflectance (ATR) accessory allows the analysis of the surface properties of samples, rather than the characteristics of the entire bulk material. In this approach, the infrared (IR) signal penetrates only about 1-2 micrometers into the sample's surface.
In this study, FTIR spectroscopy was performed using a PerkinElmer Spectrum Two spectrometer to analyze the samples by tracking changes in peaks corresponding to various functional groups. It was used in reflection mode, with a resolution of $1cm^{-1}$, four scans for each spectrum, in the wavenumbers range defined before. Before starting the measurement, it is crucial to perform an acquisition without the sample to create the "background". This background spectrum is then subtracted from the spectra acquired from the samples, and this ensure that all the spectra have the same baseline.

3.3.3 Tensile and compression test

The tensile test was performed, using a Z5 Single Column Tensile Machine with a $500N$ load cell, to evaluate the mechanical properties of the materials. The machine extends vertically and includes two grips: one fixed at the base and another movable along a vertical carriage operated by a motor for vertical movement. Each grip consists of two plates that can be tightened or loosened using specific knobs. By clamping the sample between the plates of the two grips, it can be securely held for tensile testing. The applied force (F) is measured by a load cell positioned on the movable grip (setup shown in figure 3.13).
The data are extracted from software called THSSD by Gripsoft, where it is possible to input the length, width, and thickness of the sample, in this way it is possible to obtain the corresponding stress value from the formula $\sigma = F/A$, where A is the section of the sample (the multiplication of width and thickness). Before starting the test, zero position is set and the initial length of the sample is taken (l_0), in this way it is possible to calculate also the strain (ϵ), knowing the position of the movable grip (l) with the formula $\epsilon = (l - l_0)/l_0$. Stress-strain curves were plotted to calculate the mechanical parameters of the sample. The slope of the first part of the curve represented the Young's modulus or elastic modulus.
The tensile speed was set at 5 mm/min and three types of measurements were performed:

1. Breaking tests: involved applying intentionally high values of maximum

deformation and force to the sample to induce breakage, in this way it is possible to evaluate fracture elongation and fracture tension at the point of sample breakage.

2. Durability tests: were conducted weekly over a specified period, where the sample underwent a maximum deformation equal to 20% of its initial length, assessing its performance over time.

3. Hysteresis tests: consists of cyclically stretching the sample. Initially, the sample is at rest, and then it undergoes maximum elongation equal to 20% of its initial length for a specified number N of cycles determined by the operator.

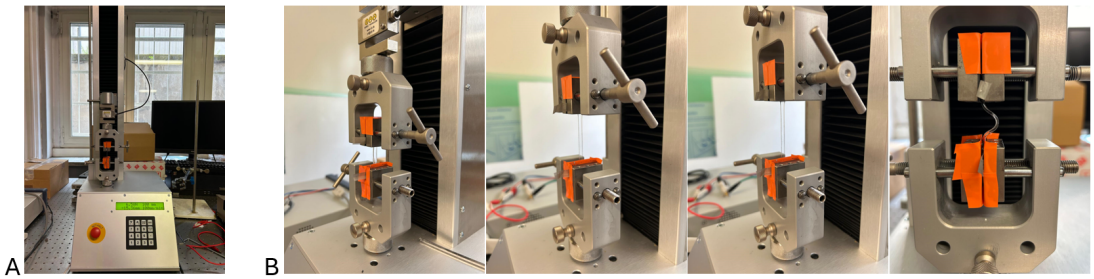

Figure 3.13: Tensile test. A) Tensile test setup, and B) Extension of a sample during a tensile test.

For the compressive test the compression speed was set at 1 mm/min and the sensor underwent a deformation of 50%, compression test setup is shown in figure 3.14.

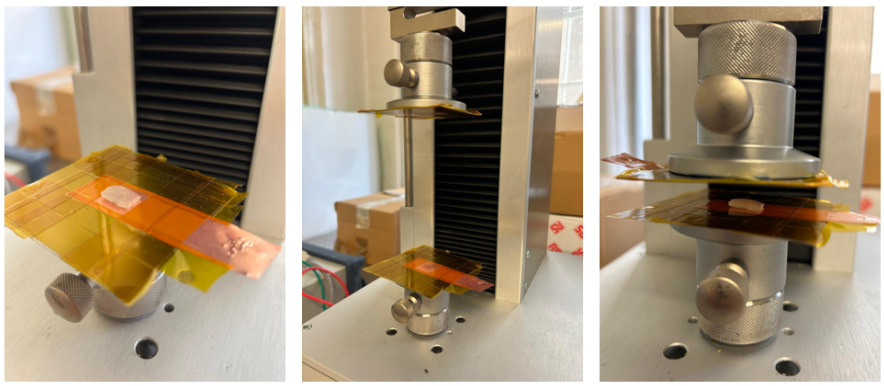

Figure 3.14: Compression test setup.

3.3.4 Electrical test

An LCR meter (BK Precision 894) was utilized to investigate the resistance variations under external deformation (setup is shown in figure 3.15A). Parameter settings and data collection were managed via LabView (National Instruments). The initial parameters set for the measurement were the stimulation frequency, fixed at 1000 Hz, and the voltage, set at 50 mV and 1 V. These settings were chosen to observe how impedance behaved under different voltage conditions. The impedance was modelled as a parallel combination of a resistor and a capacitor, as illustrated in figure 3.15B. An alternating voltage was employed to prevent the accumulation of NaCl ions on the electrodes, which would occur if a direct current were used. Indeed, when a direct current (DC) is applied to an electrolytic solution, cations and anions migrate towards the opposite electrodes. This can lead to the accumulation of ions at the electrodes, resulting in the formation of an electrical double layer and potential electrode polarization. Such accumulation can affect the electrical properties of the sensor, leading to inaccurate measurements.
The electrical test was conducted simultaneously with the tensile test, monitoring both resistance and capacitance as a function of the sensor's elongation. By combining the results from these two tests, the sensitivity can be calculated as the slope of the $\Delta R/R$ vs. ϵ curve.

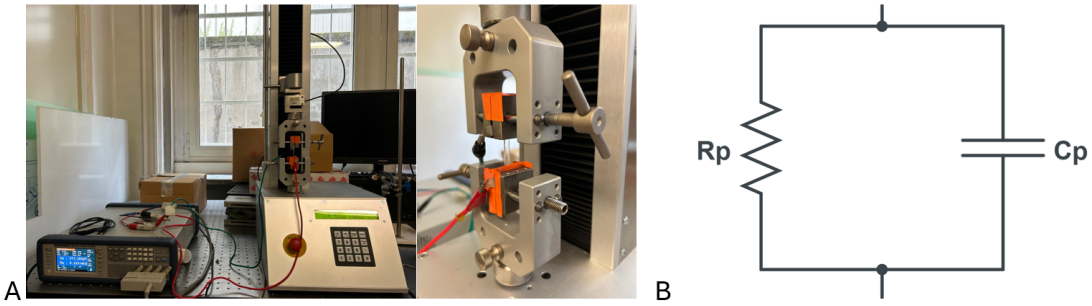

Figure 3.15: Electrical test. A) Electrical test setup, and B) Model of the impedance, consist of a parallel between a resistor and a capacitor

Chapter 4

Results and discussion

4.1 Material characterization

4.1.1 Degree of methacrylation using formaldehyde (DOF)

To conduct the test, a protocol commonly used for bovine gelatin was employed, which had demonstrated excellent linearity between 0 mg/ml and 1 mg/ml, allowing for the construction of an accurate calibration curve.
However, unlike bovine gelatin, fish gelatin is less reactive because it has fewer amino groups at the ends of the chain. As a result, bovine gelatin tends to have a higher gelling strength compared to fish gelatin. Additionally, fish gelatin gels at lower temperatures than bovine gelatin, which starts to gel at around 18°C.
At the tested concentrations, we encountered noise, likely due to the limited presence of amino groups, which prevents formaldehyde from reacting adequately. Consequently, the fluorescence test conducted on formulations with various concentrations (specified in Chapter 3.2.1) showed similar results.
To address this issue, we increased the concentration of fish gelatin to 10 mg/ml. At this concentration, the fluorescence value began to rise significantly, becoming an order of magnitude higher than that of PBS and the lower concentrations.

4.1.2 Citocompatibility test

The cytocompatibility test uses HaCaT cells, which are of interest because they reside on the outer layer of epithelial tissue. Since the sensor will be applied on the skin, this test is essential for evaluating whether the sensor could cause adverse effects at the epithelial level.
An initial solution was prepared with a 1:4 ratio of water and glycerol (one part water to four parts glycerol), containing 1M sodium chloride (NaCl) and dissolved

with 20% w/v GelMA (20 mg GelMA per 1 mL solution). Subsequently, a photoinitiator was added at 2% weight relative to GelMA (2 mg of photoinitiator per 100 mg GelMA). While TPO-SDS was previously used, its known non-biocompatible characteristics led to the use of LAP, a biocompatible photoinitiator, in this case. From this initial solution, three solutions with varying citric acid concentrations were prepared, expressed as weight percentage relative to GelMA: 0%, 20%, and 50% w/w citric acid (CA). For each formulation, four squares were polymerized using UV light, and their cytocompatibility was analyzed.
Hydrogels without citric acid demonstrated excellent cytocompatibility from the onset. In contrast, the solution with 50% w/w CA initially tested led to cell death, likely due to the acidic environment created by the citric acid. The following sections detail the results.
In our research, various cell cultures were prepared by immersing hydrogel samples with different concentrations of citric acid (0%, 20%, and 50%) in a culture medium along with other additives specified in Chapter 3.2.2. These cultures were maintained for 72 hours at a temperature of 37°C. The cell culture containing the GelMA hydrogel sample without citric acid (0% CA) was designated as the "control" and was primarily used to verify how cell viability varies with citric acid concentration, excluding influences from the base composition of the hydrogel. Additional cell cultures were prepared with GelMA hydrogel containing 20% and 50% citric acid. Moreover, an additional control, referred to as "plate," was introduced, in which initially no GelMA hydrogel was immersed.

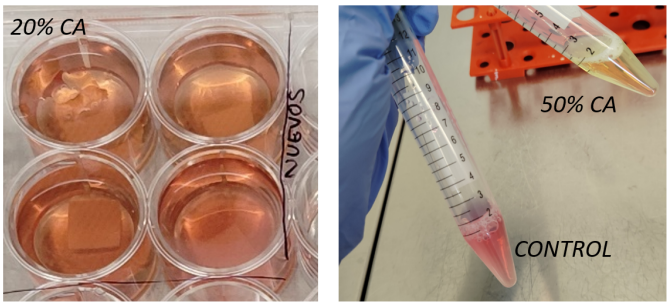

Figure 4.1: Different colour of the culture medium

These culture media exhibit different colors depending on the acidity of the medium itself, due to the presence of DMEM, a medium that changes color based on the pH of the solution: yellow for acidic pH, fuchsia for basic pH, and pink for neutral pH. In the figure 4.1, we can see that the solution in which the 50% CA sample was immersed is yellow (indicating the most acidic pH), while the solution in which the 20% CA sample was immersed appears more orange, indicating a higher pH.
Two tests were performed on these culture media: the live/dead assay and the

MTT assay, at one and three days from the start of the cell culture.
The live/dead assay is a test used to assess cell viability (Fig. 4.2). The results display the different cell cultures using hydrogel with various citric acid concentrations, at one and three days from the start of the culture. In this test, live cells appear green, while dead cells appear red.

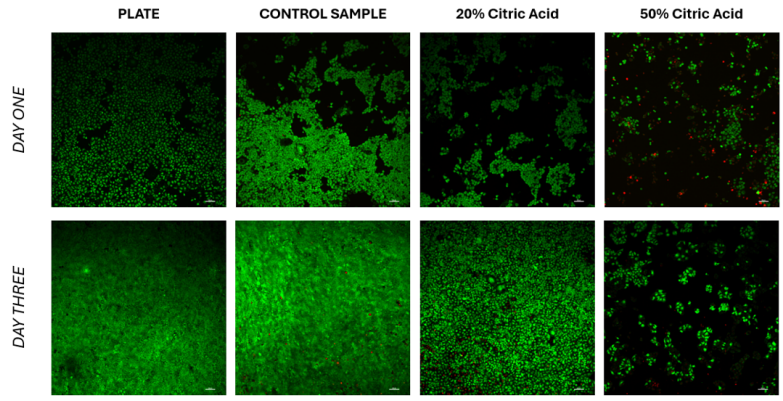

Figure 4.2: Live/dead assay used to assess cell viability

The MTT assay provides quantitative results, presented as the mean with the corresponding standard deviation of several cell cultures conducted with samples containing different concentrations of citric acid (Fig. 4.3). The differences between the various means were analyzed using the Student's t-test for independent samples, with the number of asterisks indicating the statistical significance of these differences.

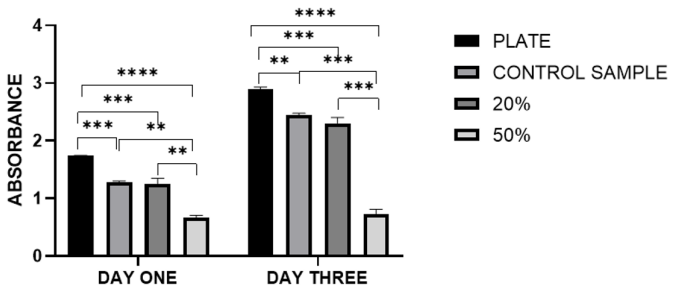

Figure 4.3: Results of the MTT assay

The Student's t-test for independent samples, also known as the unpaired two-sample t-test, is a statistical technique used to compare the means of two independent groups and determine if there is a significant difference between them.

4.2 Hydrogel and sensor characterization – Impact of Citric Acid

4.2.1 % Gel

To assess the gel content, two formulations were tested: one without citric acid (results on the table in figure 4.4) and one with 20% w/w citric acid (results on the table in figure 4.5) relative to GelMA (20 mg of CA per 100 mg of GelMA). Four samples were analyzed for each formulation.
The gel content results for both formulations were remarkably high, with all samples showing values exceeding 96%. This high percentage indicates a high degree of crosslinking within the material, reflecting effective polymerization and indicating that the unpolymerized fraction dissolved in chloroform is minimal, less than 4%. A high gel content suggests that the hydrogel network is well-formed and stable, which is crucial for applications requiring robust and resilient hydrogels. Both formulations exhibited similar results, suggesting that citric acid, at the tested concentration, does not influence the crosslinking efficiency or the structural integrity of the hydrogels. This finding is crucial as it implies that citric acid can be included for its other potential benefits or functionalities without compromising the fundamental cross-linking characteristics of the hydrogel network.

Sample	Weight of the sample (mg)	Weight of the lab net (mg)	Initial total weight (mg)	Final total weight (mg)	%Gel (%)
Sample 1	149,72	747,22	896,94	896,37	99,61928934
Sample 2	199,11	1199,33	1398,44	1394,2	97,87052383
Sample 3	155,25	1365,19	1520,44	1515,28	96,6763285
Sample 4	163,25	1206,52	1369,77	1367,47	98,59111792

Figure 4.4: Table of %Gel results in samples without citric acid

Sample	Weight of the sample (mg)	Weight of the lab net (mg)	Initial total weight (mg)	Final total weight (mg)	%Gel (%)
Sample 1	155,49	1157,48	1312,97	1310,2	98,21853495
Sample 2	219,45	919,5	1138,95	1133,31	97,42993848
Sample 3	231,48	1612,65	1844,13	1842,4	99,25263522
Sample 4	266,85	1436,92	1703,77	1702,25	99,43039161

Figure 4.5: Table of %Gel results in samples with 20% w/w citric acid

4.2.2 FTIR-ATR spectroscopy

In the analysis of the hydrogel composed of methacrylated gelatin and citric acid, spectroscopy has provided valuable insights into its molecular composition and structure. Various spectral peaks have been identified across different regions of the infrared spectrum, each revealing specific chemical bonds and functionalities present

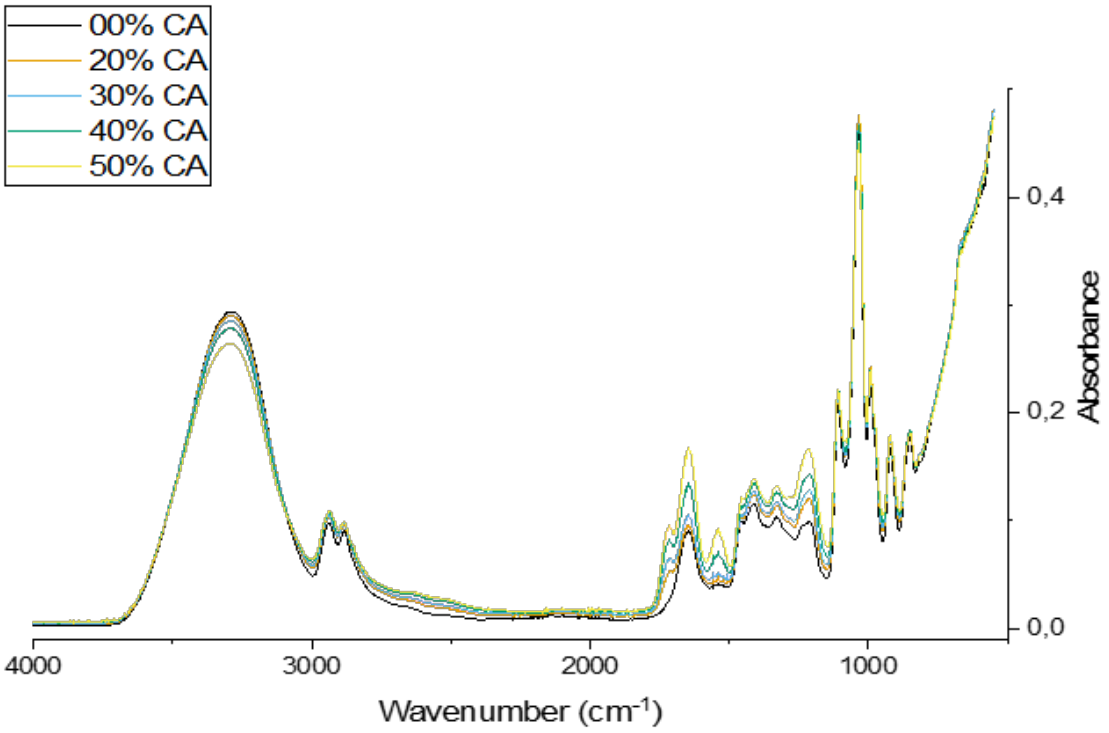

Figure 4.6: FTIR-ATR spectroscopy results of samples with different concentration of citric acid

within the material. In figure 4.6, the absorbance spectra of various GelMA samples (20% w/v, 20 mg of GelMA in 1 mL of solution) with different concentrations of citric acid (ranging from 0% w/w to 50% w/w relative to the weight of GelMA) are depicted. Specifically, recurring peaks are observed.
At 3346 cm^{-1}, prominent stretching vibrations of O-H and N-H bonds were observed, indicative of hydrogen bonding interactions within the gelatin backbone. This highlights the presence of hydrophilic groups essential for water retention and biocompatibility in biomedical applications.
The spectral range of 2800–3100 cm^{-1} exhibited stretching vibrations of C-H bonds, which are characteristic of the alkyl groups present in the methacrylated gelatin structure. These bonds contribute to the overall stability and structural integrity of the hydrogel.
Between 1651-1544 cm^{-1}, distinct peaks were observed corresponding to various stretching and bending vibrations: C=O stretching, coupled N-H bending with C-H stretching, and C-N stretching with N-H bending. These peaks provide evidence of the chemical modifications introduced during the methacrylation process.
A significant peak at 1651 cm^{-1} specifically indicated the conversion of C=C double

bonds typically found in methacrylate groups. This transformation underscores the successful incorporation of methacrylate functionalities into gelatin.
Further characterization of the absorbance spectrum between 1500 cm^{-1} and 1100 $cm^{-}1$ revealed additional structural details that are always present in gelatin's spectroscopy:

- Around 1450 cm^{-1} there is the deformation vibrations of aromatic rings.
- At approximately 1400 cm^{-1}, deformation vibrations of C-H bonds in aromatic groups further corroborate the presence of aromatic functionalities within the hydrogel.
- Vibrations around 1300 cm^{-1} predominantly stemmed from C-H bonds in methyl and methylene groups, contributing to the overall flexibility and mobility of the gelatin chains.
- Peaks around 1200 cm^{-1} indicated vibrations of C-O-C and C-N bonds.

Examining various concentrations of citric acid reveals distinct peaks around 1720 and 1650 cm^{-1}, each with specific implications:

- The peak at 1650 cm^{-1} typically corresponds to stretching vibrations of N-O bonds, suggesting that the presence of citric acid may alter the structural properties of gelatin, potentially increasing chain flexibility.
- The peak at 1720 cm^{-1} usually indicates stretching vibrations of C=O bonds, characteristic of citric acid itself. Therefore, the addition of citric acid can indeed create this spectral feature.

These findings highlight the significant impact of citric acid on the structure and properties of gelatin-based materials, potentially affecting their mechanical and chemical characteristics.

4.2.3 Tensile and electrical tests

Compressive and tensile tests were conducted on samples formulated as follows: 20% w/v GelMA (20 mg GelMA per 1 mL of solution) in a mixture of water and glycerol in a 1:4 ratio (1 part water to 4 parts glycerol), with 1 M sodium chloride and 2% w/w TPO relative to GelMA (2 mg TPO per 100 mg GelMA). To this solution, varying amounts of citric acid were added, denoted as "XX CA" where "XX" represents the concentration of citric acid in weight percent relative to GelMA (XX mg of citric acid per 100 mg of GelMA): 00 CA, 20 CA, 30 CA, 40 CA, and 50 CA.
Regarding the compressive tests, the stress-strain curves show that samples with

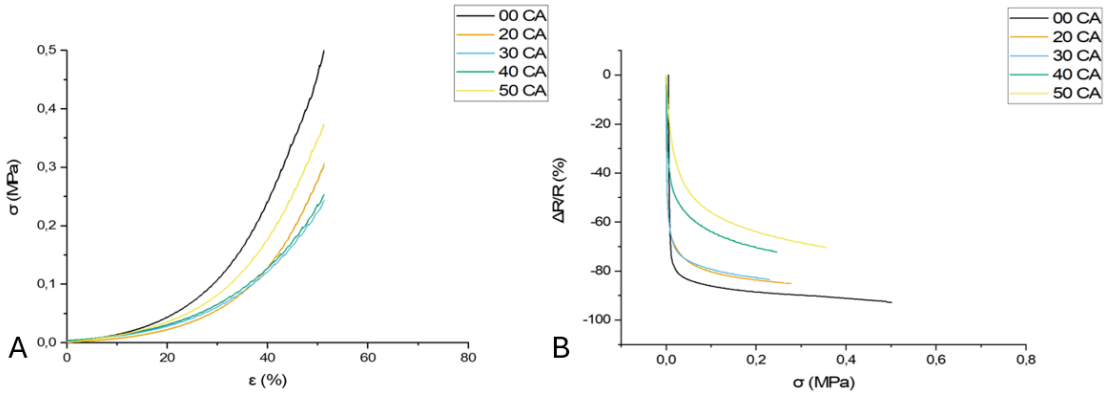

Figure 4.7: σ-ϵ compression curves (A) and $\Delta R/R$-σ compression curves (B) of samples with different concentration of citric acid

different concentrations of citric acid respond similarly (as depicted in Figure 4.7). However, in terms of $\Delta R/R$-σ curves, it appears that at the same level of deformation, the $\Delta R/R$ decreases with increasing citric acid concentration.
In addition, tensile tests to failure, durability tests, and hysteresis tests were also conducted on dog-bone-shaped samples.
In tensile tests to failure (Fig. 4.8A), it can be observed that the presence of citric acid decreases the slope of the linear region in the stress-strain curve, indicating a reduction in the Young's modulus (Fig. 4.8B).

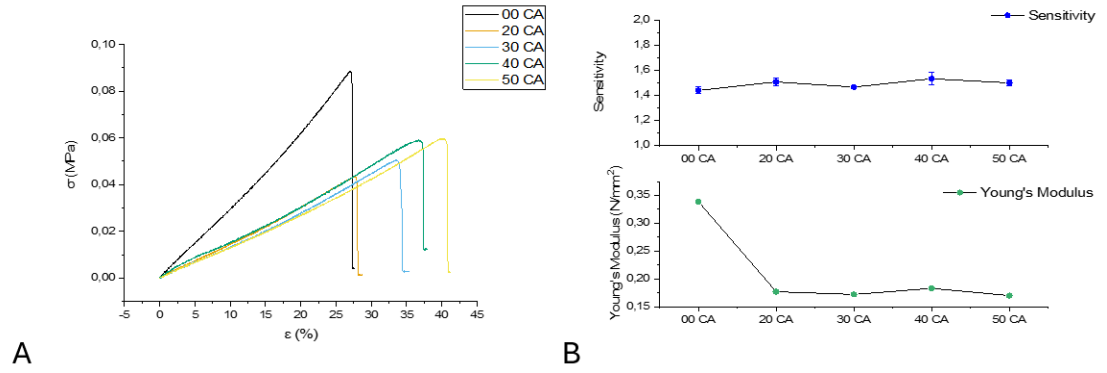

Figure 4.8: σ-ϵ tensile tests to failure curves (A) and sensitivity and Young's modulus values (B) of samples with different concentration of citric acid

Simultaneously, as the concentration of citric acid increases, the maximum strain before failure also increases. Starting from a maximum strain of 27% in the sample without citric acid, it reaches a maximum strain of 42% with 50% citric acid concentration.

From the $\Delta R/R$-ϵ curves, the sensitivity value was derived as the slope of the curve, which remains nearly constant across varying concentrations of citric acid (Fig. 4.8B).
Durability tests were conducted on samples without citric acid and samples with 20% citric acid. In all samples, a maximum deformation of 20% was applied, and sensitivity and Young's modulus were monitored over time. The samples were kept in Petri dishes without Parafilm or other special conditions to assess their durability under ambient environmental fluctuations, without specific attention to refrigeration or constant humidity and temperature control. The durability test spanned a total of 70 days.

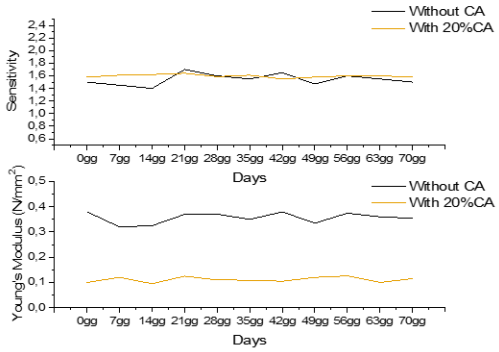

Figure 4.9: Sensitivity and Young's modulus values of samples during the 70-days durability test on samples with different concentration of citric acid (0% and 20%)

Over time, minor variations were observed in the measured parameters, which were not attributed to wear or elapsed time but primarily to fluctuations in ambient temperature and humidity. However, it is notable that the curves corresponding to formulations with citric acid exhibited greater stability throughout the testing period (Fig. 4.9).

The final tensile test performed on the samples was the hysteresis test. In this test, the samples were cyclically deformed to 20% of their initial length and then returned to the original length, completing a total of 30 cycles to evaluate hysteresis (Fig. 4.10).
Studying the hysteresis curve is crucial for understanding the material's behavior, which helps in enhancing material design and predicting performance. This knowledge is essential to ensure the reliability and durability of the final products.
The deformational response of the material under loading and unloading does not follow the same path, resulting in a closed-loop curve; the enclosed area represents the energy dissipation. In this case, the material exhibited viscoelastic behavior, where deformation is time-dependent and related to the loading. However, the

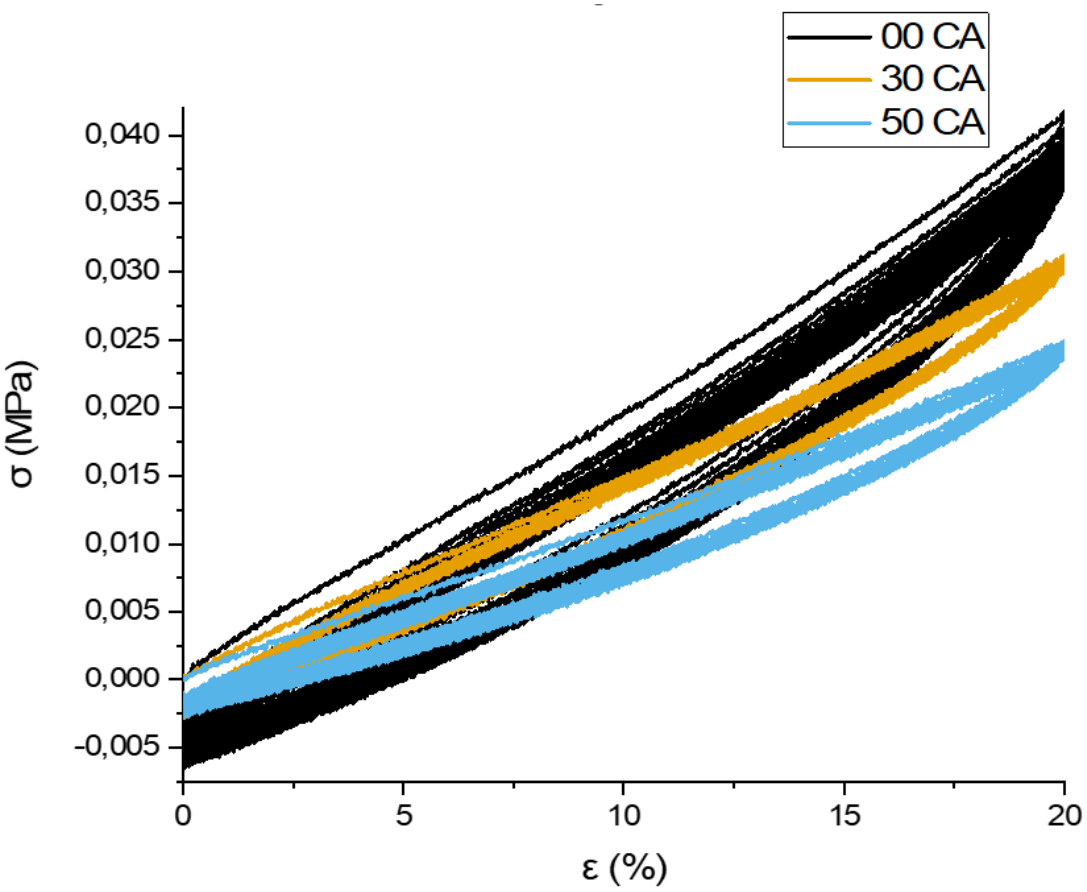

Figure 4.10: Stress-strain curve between the sample without citric acid and with 30% and 50% w/w of citric acid

deformation was transient and fully recovered shortly after the removal of the load. It can be observed that in the case of the 50CA sample, the material can withstand repeated cycles without significant alterations in the applied load from cycle to cycle. In contrast, the continuous downward shift of the hysteresis curve observed in the 00CA sample indicates that the material is progressively "yielding" under the applied load. In other words, the deformation resistance of the 00CA sample tends to decrease over time under repeated loads probably due to the relaxation of the polymer matrix.

To complete the hysteresis study of the material, the impedance of the material was also measured during the test (Fig. 4.10). The impedance is represented, as previously mentioned, by a resistance and a capacitance in parallel. It is observed that in the case of the 00CA sample, the resistance shows a downward trend, reflecting the decrease in internal strength due to viscoelastic relaxation. This

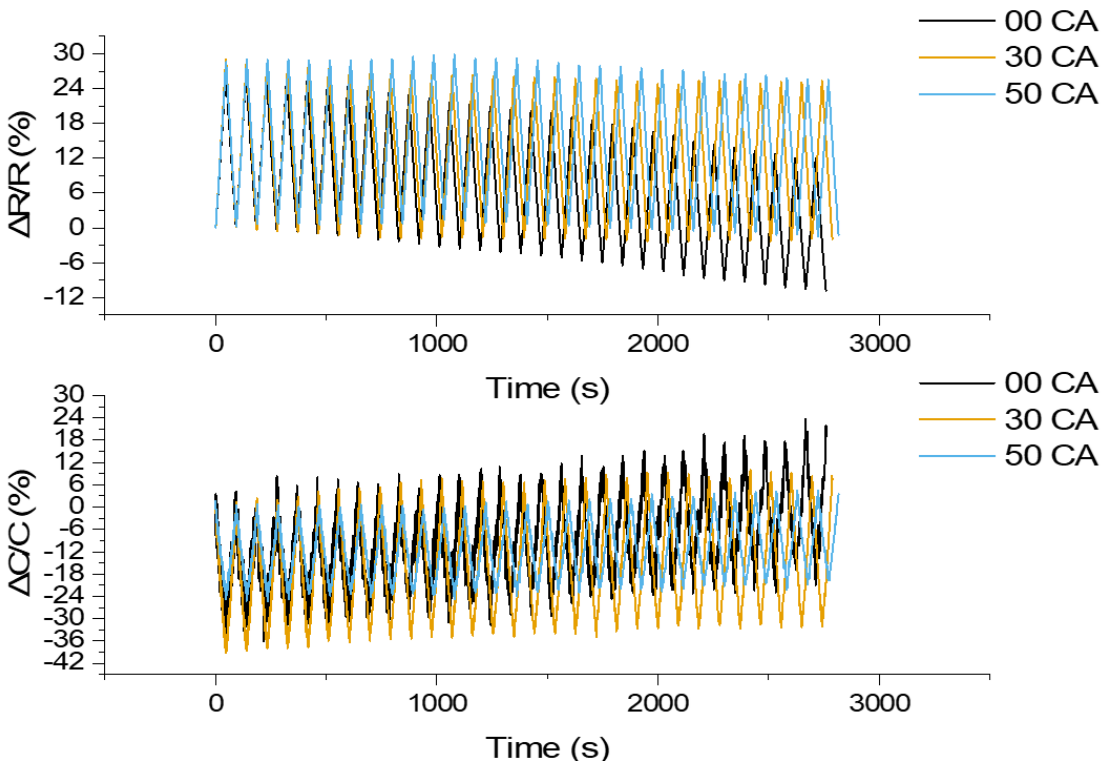

Figure 4.11: The difference in the $\Delta R/R$-time and $\Delta C/C$-time curves between the samples without citric acid and with 30% and 50% w/w of citric acid

phenomenon is virtually absent in the 50CA sample, which maintains a constant resistance.
At the same time, it can be observed that the material is also very sensitive concerning capacitance, with the capacitance curve being much less noisy in the case of the 50CA sample. This indicates that capacitance can be an effective measure for monitoring material deformation. Therefore, the study of material deformation can be conducted not only by using the variation in resistance but also by the variation in capacitance. The lower noise in the capacitance curve of the 50CA sample facilitates a more precise analysis, making capacitance a useful variable for evaluating the viscoelastic behaviour and stability of the material under cyclic loads.
In conclusion, it can be observed that increasing the concentration of citric acid can contribute to making the polymer matrix of GelMA more compact, which enhances mechanical stability and reduces viscoelastic relaxation. As highlighted in the samples studied, the presence of citric acid led to a lower downward shift of the hysteresis curve, suggesting better resistance to deformation under repeated loads. Therefore, optimizing the concentration of citric acid can be crucial to improve the

mechanical properties and durability of GelMA hydrogels.

4.2.4 Temperature dependency of resistance

During a 70-day period, resistance measurements were acquired from various samples stored in Petri dishes at room temperature throughout the testing period. The tests were conducted on samples without citric acid because, as will be explained later, the resistance variation was the same for samples with CA as for samples without CA.
It was observed that the resistance varied randomly among all samples, rather than correlating with the duration of use, as might be expected due to potential evaporation of the aqueous component in the sensor.
In response to these observations, knowing the glycerol's sensitivity to temperature and humidity fluctuations, environmental values were logged during the experiments. A graph was constructed adding humidity and temperature on the y-axes (Fig. 4.12), revealing significantly higher resistance values when the temperature dropped below 18°C. This is attributed to glycerol's melting point at 18.17°C; when the temperature falls below this threshold, glycerol may undergo a phase transition between solid and liquid states, leading to a notably increased viscosity compared to its liquid state. Consequently, this viscosity increase impedes the movement of NaCl ions, thereby resulting in higher electrical resistance.
In order to conduct a more targeted study in the impact of temperature on the material's resistance, tests were conducted by placing the sample inside a constant humidity oven and incrementally increasing the temperature. The resistance was evaluated approximately every 5°C using an LCR meter connected to the sample inside the oven (Fig. 4.13). This approach allowed for the construction of a curve by interpolating the collected data points:

$$y = 134{,}83307 * e^{-\frac{x}{11{,}55764}} + 10{,}68822 \tag{4.1}$$

4.3 Hydrogel and sensor characterization – Impact of Tannic Acid

Finally, further studies were conducted on a formulation of 20% w/v GelMA (20 mg of GelMA per 1 mL of solution) in a mixture consisting of 1:4 ratio of water to glycerol (1 part water to 4 parts glycerol) and 1 M NaCl, into which tannic acid was introduced by immersing the sample in a solution of tannic acid and water at a ratio

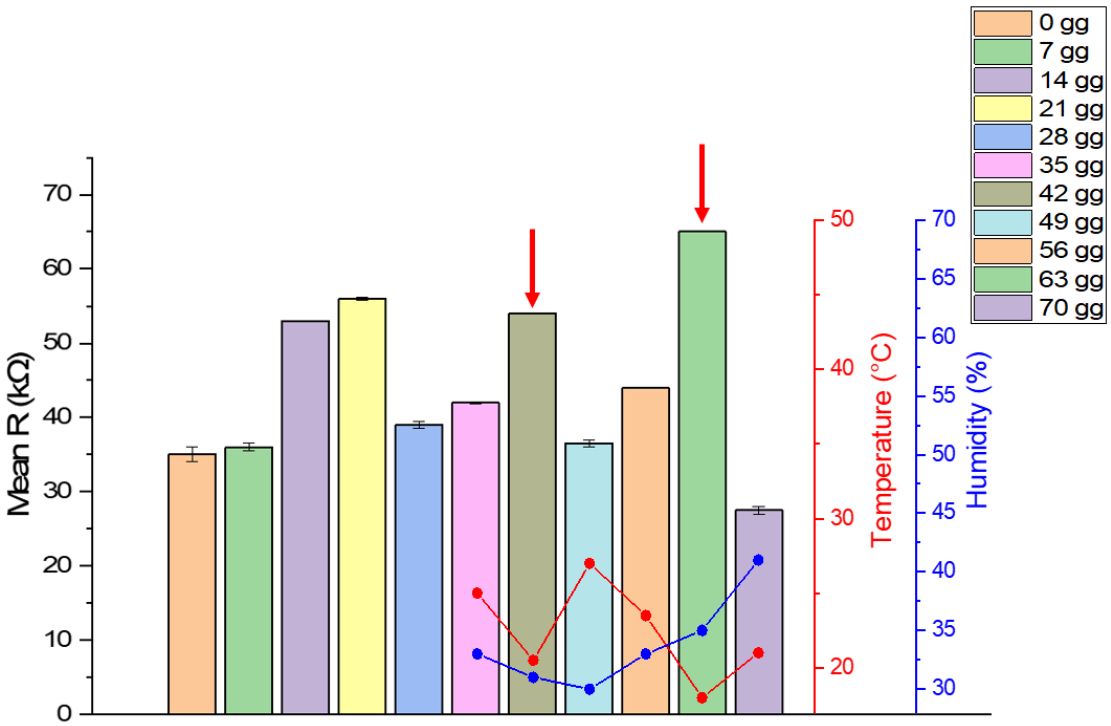

Figure 4.12: The variation of resistance during the 70-days period and the variation of resistance with some registered temperature and humidity on sample without citric acid

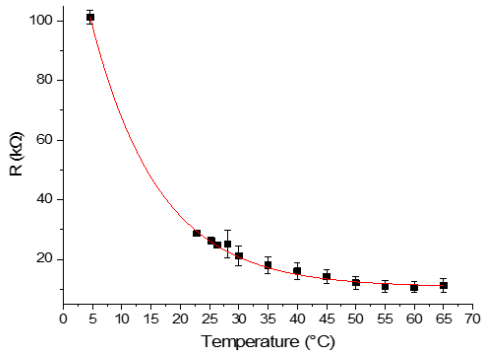

Figure 4.13: The variation of resistance during the test conducted inside the oven on sample without citric acid, with 20% w/w, 30% w/w, 40% w/w and 50% w/w of citric acid

of 2:3 (two parts tannic acid to three parts water) for varying durations. Samples were prepared by immersion for 1h, 3h, 5h, 9h, and 15h, denoted for convenience as

"xh TA" with x representing the immersion time in hours. It was observed that the dog-bone shaped sample dimensions decreased proportionally with the immersion time, as shown in Figure 4.14A, while simultaneously the resistance increased (Fig. 4.14B).

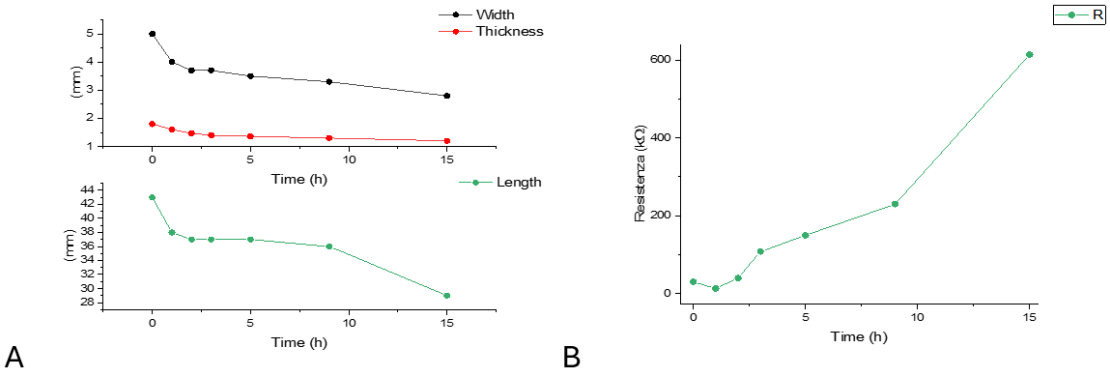

Figure 4.14: Dimensions (A) and resistance (B) of samples immersed in tannic acid solution for different amount of time

After preparing the samples, their absorbance FTIR-ATR spectroscopy was evaluated (Fig. 4.15), resulting in the graph shown in the figure. It can be observed that as the immersion time increases, the typical characteristics exhibited by a gelatin hydrogel in an absorbance spectrum, such as peaks at 2800 $cm^{-}1$ and peaks between 1100 and 1750 $cm^{-}1$, diminish.
At the same time, the presence of new peaks around 1700 $cm^{-}1$ and 1600 $cm^{-}1$ can be observed, but it was not possible to determine definitively whether these were due to aromatic components present in tannic acid or if they represented shifts in neighbouring peaks. However, a clearly visible peak at 750 $cm^{-}1$ corresponds to stretching of C=C bonds and bending of C-H bonds, both highly characteristic of tannic acid, indicating that tannic acid has indeed penetrated the hydrogel matrix.

Another significant finding indicating the incorporation of tannic acid into the matrix, as shown in fig. 4.16 is the comparison between the absorbance spectrum of the "15h TA" sample (upper figure) and that of pure tannic acid (lower figure). These spectra are nearly identical, indicating that the matrix is composed almost exclusively of tannic acid and suggesting that the gelatin has somehow been extracted from the hydrogel.
However, the samples were very rigid and difficult to test on the tensile testing machine.

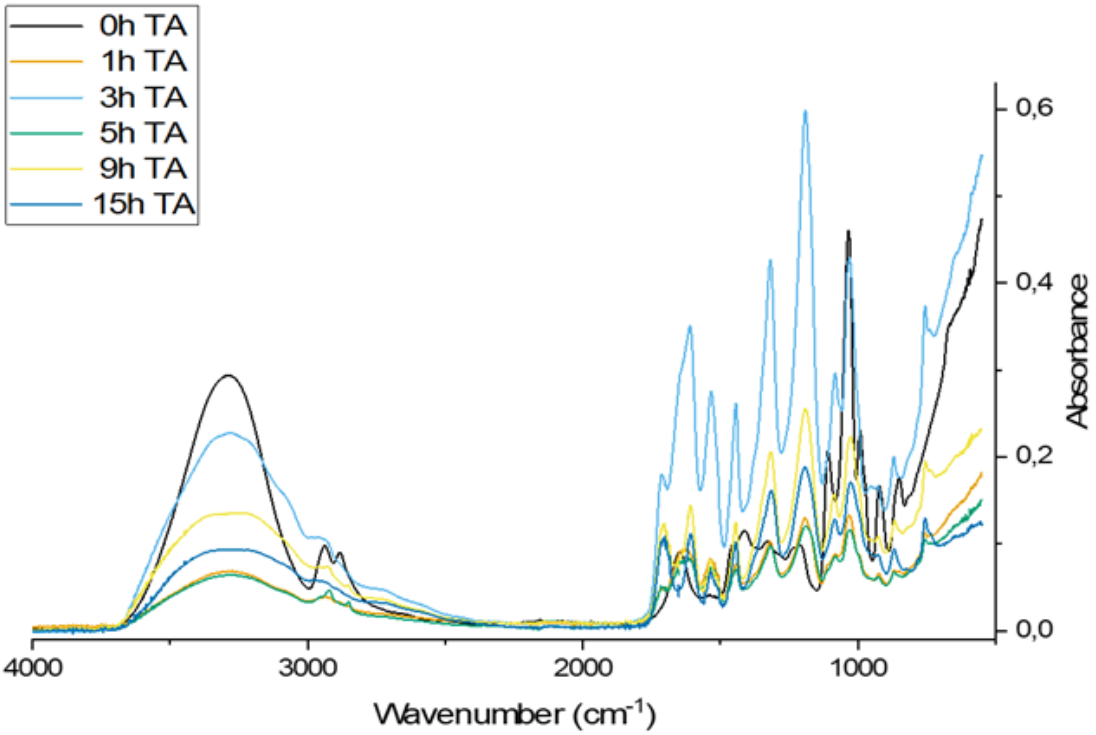

Figure 4.15: FTIR-ATR spectroscopy results of samples with different time of immersion in a tannic acid solution

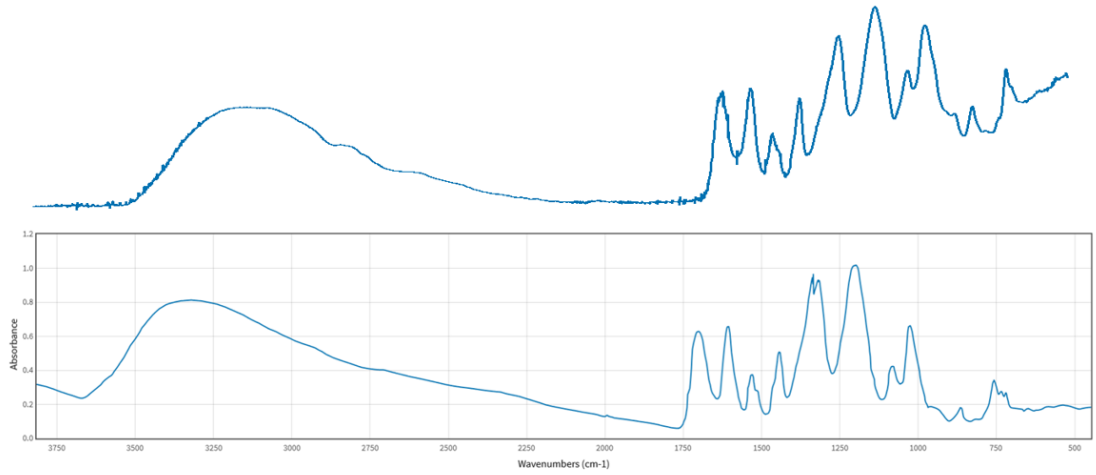

Figure 4.16: FTIR-ATR spectroscopy results of samples with 15h of immersion in a tannic acid solution

Chapter 5

Conclusions

In conclusion, this thesis aimed to enhance a sensor based on GelMA hydrogel by incorporating additives that improve its electrical, mechanical, and durability properties while maintaining its inherent biocompatibility. Notably, excellent results were achieved through the integration of glycerol and citric acid.
Glycerol, being less volatile, remains within the matrix at elevated temperatures, providing flexibility and resilience to the hydrogel even under challenging operational conditions. Glycerol's higher viscosity and lower vapor pressure compared to water reduce the rate of evaporation, enhancing the material's mechanical stability. Moreover, glycerol is an effective ionic conductor, and this improve the material's electrical properties. Its presence in the formulation promotes better distribution and mobility of ions within the matrix, contributing to more stable and efficient electrical conductivity. The phase transition of glycerol at 18°C leads to an increase in viscosity, which hinders the movement of NaCl ions and consequently increases the electrical resistance; to obtain more precise and reliable results, it is crucial to test the sensor under controlled temperature and humidity conditions.
The presence of citric acid shows through durability tests the diminution of the Young's modulus of crosslinked GelMA hydrogels. The incorporation of citric acid into the hydrogel matrix can lead to two main outcomes:

1. Plasticization: Citric acid acts as a plasticizer, enhancing the flexibility of the polymer network by increasing the mobility of the polymer chains. This results in a decrease in the Young's modulus, making the hydrogel softer and more deformable under applied force without compromising the degree of crosslinking.

    - Effect of pH: citric acid, being a weak acid, lowers the pH of the solution. This pH change can affect the ionization of functional groups on GelMA, a lower pH can reduce the reactivity of the methacrylic groups in GelMA,

decreasing their interaction with the photoinitiator, and for this reason, decreasing the cross-linking.

- Inhibition of Photoinitiation through interaction with TPO-SDS: citric acid might interact with TPO, affecting its ability to generate free radicals under UV light.

2. Impact on Cross-linking Efficiency: citric acid could compromise the degree of cross-linking through several effects:

Despite citric acid's potential to affect the cross-linking process, the %gel showed that the degree of cross-linking remained consistently high (over 96%). This suggests that the structural integrity of the hydrogel was maintained, even with the presence of citric acid.
In addition, the presence of citric acid shows through the hysteresis test a viscoelastic relaxation, that was evident in the observed differences in resistance behaviour between samples with varying citric acid concentrations. Increased citric acid concentration improved the mechanical stability and reduced viscoelastic relaxation, indicating a more compact and flexible polymer matrix.
When tannic acid was added to the solution without citric acid, it caused the sample to shrink, making it more fragile and drier. To continue using this method and potentially achieve interesting results, increasing the water content in the matrix or starting with a larger initial sample size before immersing it in tannic acid could be beneficial. This underscores the need for careful balance when modifying hydrogel formulations to ensure desirable mechanical properties without introducing testing complications.
Finally, regarding the DOF test to calculate the degree of methacrylation, for future studies, it would be advisable to start with concentrations higher than 10 mg/ml in order to achieve a more precise and reliable calibration curve.
To conclude the study, in vivo tests were conducted using the developed sensors on various body parts to evaluate the impact of deformation on the measured resistance. The following images illustrate the obtained results (Fig. 5.1 and Fig. 5.2).

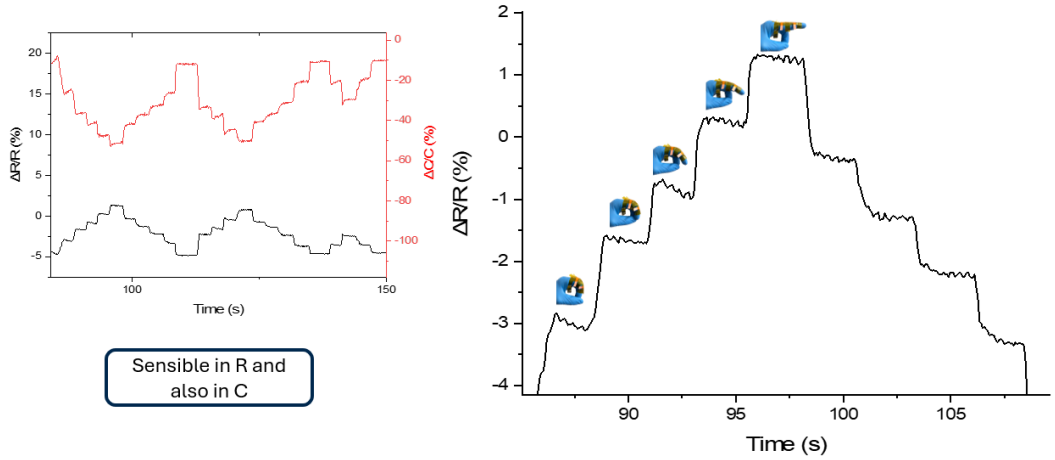

Figure 5.1: Finger bending monitoring – Resistance and capacitance signal in reaction to different bending angles

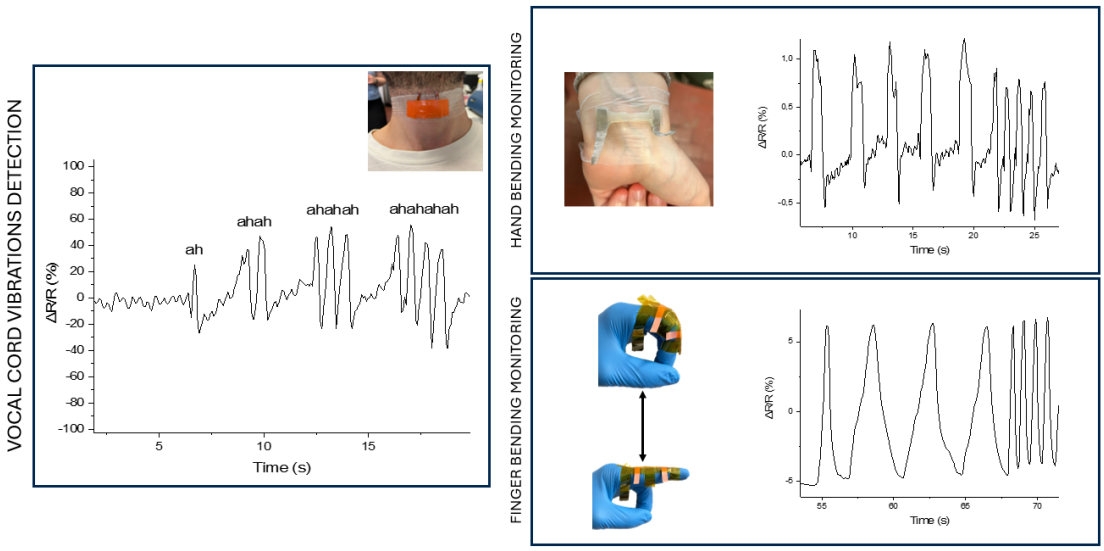

Figure 5.2: Vocal cord vibrations detection, hand bending monitoring, and finger bending monitoring

Future studies and future applications

Future studies could continue this research by investigating new additives or adjustments to customize GelMA hydrogels for specific biomedical uses. Optimizing preparation methods and gaining a deeper understanding of how chemical components interact are crucial steps toward effectively integrating GelMA-based materials into practical applications.

Enhanced study of sensor response to temperature and humidity changes

To make GelMA-based strain sensors even better, it is important to study how they perform in different temperatures and humidity. One big focus should be on how these sensors react to changes in temperature. The temperature response has been studied before, but we still need to delve deeper into how the material reacts when temperatures change while keeping humidity levels constant. This research aims to clarify how temperature variations interact with consistent humidity conditions, giving us a better understanding of how the material performs in different environmental setups.

At the same time, it is also important to studying how different humidity levels affect the sensor. The sensor could be tested in a controlled environment to observe how humidity interferes with the material properties.

By combining these two studies, it is possible to observe how the sensor behaves and maybe introduce additives or modifications to ensure its performance remains stable across varying temperatures and humidity levels. Similarly, by combining these two studies, it might be possible creating a temperature and humidity compensation algorithm to correct for environmental variations in real-time applications.

Targeted Studies on the Impact of Citric Acid on Cytocompatibility

Future research should study how citric acid affects the compatibility of GelMA hydrogels, especially its interactions with cells. One big area to focus on is checking how cells respond when exposed to different amounts of citric acid mixed into the hydrogel. It's crucial to use a variety of cell types to get a full picture of how well citric acid works in GelMA hydrogels.

It's also important to understand how citric acid interacts with cells at a molecular level. Using advanced techniques can help us see how citric acid changes what's happening inside cells within the hydrogel. At the same time, experiments need to be conducted for extended periods to observe how cells continue to respond to citric acid over time.

All this research will give a solid grasp on how citric acid influences the GelMA hydrogel's ability to work well with cells. Ultimately, this knowledge will be useful for creating hydrogel systems that are not only more effective but also safer for biomedical uses.

Sensor Integration for Cell Cultivation

The integration of GelMA-based strain sensors within cell culture systems holds significant potential for providing real-time monitoring of cellular activity and mechanical forces. Future advancements in this area should concentrate on several key aspects to fully realize this potential.

Firstly, it's crucial to monitor the cellular environment closely. By integrating these sensors into bioreactors or cell culture platforms, we can measure the mechanical

stresses and strains that affect cells. This real-time data helps us better understand how cells behave and respond, which is key for advancing in tissue engineering and regenerative medicine. By studying how cells react to different mechanical forces, researchers can optimize conditions to promote better cell growth and tissue development.
Equally important is the design of the sensors to ensure biocompatibility. This includes assessing the potential for any substances or degradation products that may be released from the sensors and could potentially harm cell health. Minimizing these risks is crucial to preserving the integrity of cell cultures and ensuring reliable data collection.

Integration of the Sensor in Prosthetics and Orthoses
Integrating GelMA-based strain sensors into prosthetic and orthotic devices can significantly enhance their functionality and user experience, especially considering that the durability and longevity of the sensor materials are crucial for their successful application.
A primary focus should be on developing customized sensor configurations that fit in the patient-specific geometries of prothesis and orthosis. This means that it is important to design sensors that accommodate various placement options, sizes, and form factors to optimize performance while maintaining the comfort and functionality of the devices. Considerations should include the sensor's attachment method to ensure that it integrate smoothly without impeding the device's usability or causing discomfort to the user.
Overall, incorporating these sensors into real-time feedback systems is essential for enhancing the adaptive capabilities of prosthetics and orthotics. These feedback systems would provide continuous data on mechanical stresses, alignment, and user movements, enabling dynamic adjustments based on user activity and changing environmental conditions. This could significantly improve the responsiveness and functionality of prosthetic limbs, allowing for more natural and effective movement.

Overall, advancing the study of GelMA-based strain sensors through these avenues will not only enhance their performance and applicability but also broaden their potential impact in biomedical engineering and healthcare.

Bibliography

[1] Angela S Mao and David J Mooney. «Regenerative medicine: Current therapies and future directions». In: *Proceedings of the National Academy of Sciences* 112.47 (2015), pp. 14452–14459 (cit. on p. 1).

[2] Ranjeet Singh Mahla. «Stem Cells Applications in Regenerative Medicine and Disease Therapeutics». In: *International Journal of Cell Biology* 2016 (2016), Article ID 6940283 (cit. on p. 2).

[3] Chris Mason and Piers Dunnill. «A Brief Definition of Regenerative Medicine». In: *Regenerative Medicine* 3.1 (2008), pp. 1–5 (cit. on p. 2).

[4] A. Iovene, Y. Zhao, S. Wang, and K. Amoako. «Bioactive Polymeric Materials for the Advancement of Regenerative Medicine». In: *Journal of Functional Biomaterials* 12.1 (2021), p. 14 (cit. on p. 3).

[5] Aja Aravamudhan, Daisy M. Ramos, Ahmed A. Nada, and Sangamesh G. Kumbar. «Natural Polymers: Polysaccharides and Their Derivatives for Biomedical Applications». In: *Natural and Synthetic Biomedical Polymers*. Elsevier, 2014, pp. 67–89 (cit. on p. 3).

[6] J. Alipal, N.A.S. Mohd Pu'ad, T.C. Lee, N.H.M. Nayan, N. Sahari, H. Basri, M.I. Idris, and H.Z. Abdullah. «A review of gelatin: Properties, sources, process, applications, and commercialization». In: *Materials Today: Proceedings* 42 (2021), pp. 240–250 (cit. on p. 3).

[7] Yun Piao, Hengze You, Tianpeng Xu, Ho-Pan Bei, Imanuel Zvi Piwko, Yu Yan Kwan, and Xin Zhao. «Biomedical applications of gelatin methacryloyl hydrogels». In: *Engineered Regeneration* 2 (2021), pp. 47–56 (cit. on p. 4).

[8] Jirong Yang et al. «A mechanical-assisted post-bioprinting strategy for challenging bone defects repair». In: *Nature Communications* 15 (2024), Article number: 3565 (cit. on p. 4).

[9] S. Jo, J. Lee, H. Lee, et al. «The one-step fabrication of porous hASC-laden GelMA constructs using a handheld printing system». In: *npj Regenerative Medicine* 8 (2023), Article number: 30 (cit. on p. 4).

[10] Sattwikesh Paul, Karsten Schrobback, Phong Anh Tran, Christoph Meinert, Jordan William Davern, Angus Weekes, and Travis Jacob Klein. «Photo-Cross-Linkable, Injectable, and Highly Adhesive GelMA-Glycol Chitosan Hydrogels for Cartilage Repair». In: *Advanced Healthcare Materials* 12.32 (2023) (cit. on p. 4).

[11] Jian Li, Yifan Lv, Zheng Chen, Jian Zhao, and Shuo Wang. «Citric Acid Loaded Hydrogel-Coated Stent for Dissolving Pancreatic Duct Calculi». In: *Gels* 10 (2024), p. 125 (cit. on pp. 5, 10).

[12] Farshad Khoshnoud and Clarence W de Silva. «Recent advances in MEMS sensor technology–biomedical applications». In: *IEEE Instrumentation & Measurement Magazine* 15.1 (2012), pp. 8–14 (cit. on pp. 5, 6).

[13] R. Ahmad and K. N. Salama. «Physical Sensors for Biomedical Applications». In: *2018 IEEE SENSORS*. IEEE. New Delhi, India, 2018, pp. 1–3 (cit. on p. 5).

[14] Yang Li, Weihua Chen, and Lehui Lu. «Wearable and Biodegradable Sensors for Human Health Monitoring». In: *ACS Applied Bio Materials* 4 (2021), pp. 122–139 (cit. on pp. 6, 23, 27–29).

[15] Nan Zhou, Tianjiao Liu, Bianying Wen, Coucong Gong, Gang Wei, and Zhiqiang Su. «Recent Advances in the Construction of Flexible Sensors for Biomedical Applications». In: *Biotechnology Journal* 15 (2020) (cit. on p. 6).

[16] E.J. Curry et al. «Biodegradable Piezoelectric Force Sensor». In: *Proceedings of the National Academy of Sciences of the United States of America* 115 (2018), pp. 909–914 (cit. on p. 6).

[17] Manuel Baumgartner et al. «Resilient yet entirely degradable gelatin-based biogels for soft robots and electronics». In: *Nature Materials* 19 (2020), pp. 1102–1109 (cit. on p. 7).

[18] Daniel Hardman, Thuruthel George, and Fumiya Iida. «Self-healing ionic gelatin/glycerol hydrogels for strain sensing applications». In: *NPG Asia Materials* 14 (2022), p. 11 (cit. on pp. 7, 10).

[19] Qi Zhang et al. «Ultrasoft and Biocompatible Magnetic-Hydrogel-Based Strain Sensors for Wireless Passive Biomechanical Monitoring». In: *ACS Nano* 16.12 (2022), pp. 21555–21564 (cit. on p. 8).

[20] Z. Li et al. «Gelatin Methacryloyl-Based Tactile Sensors for Medical Wearables». In: *Advanced Functional Materials* 30 (2020), p. 2003601 (cit. on pp. 8, 25, 26).

[21] Ximin Yuan, Pengcheng Wu, Qing Gao, Jie Xu, Bin Guo, and Yong He. «Multifunctionally wearable monitoring with gelatin hydrogel electronics of liquid metals». In: *Mater. Horiz.* 9 (2022), pp. 961–972 (cit. on pp. 8, 9).

[22] Shen Wang, Jinfeng Lei, Xueling Yi, Lun Yuan, Liming Ge, Defu Li, and Changdao Mu. «Fabrication of Polypyrrole-Grafted Gelatin-Based Hydrogel with Conductive, Self-Healing, and Injectable Properties». In: *ACS Applied Polymer Materials* 2.7 (2020), pp. 3016–3023 (cit. on p. 9).

[23] Bingcheng Liu et al. «Hydrogen bonds autonomously powered gelatin methacrylate hydrogels with super-elasticity, self-heal and underwater self-adhesion for sutureless skin and stomach surgery and E-skin». In: *Biomaterials* 171 (2018), pp. 83–96 (cit. on pp. 9, 10).

[24] Xinjie Pei, Jintao Wang, Yang Cong, and Jun Fu. «Recent progress in polymer hydrogel bioadhesives». In: *Journal of Polymer Science* 59.13 (2021), pp. 1312–1337 (cit. on p. 10).

[25] David Seliktar. «Designing cell-compatible hydrogels for biomedical applications». In: *Science (New York, N.Y.)* 336.6085 (2012), pp. 1124–1128 (cit. on pp. 11, 14).

[26] Sakshi B. Bhalerao, Vijay R. Mahajan, and Rahul R. Maske. «Hydrogel based drug delivery system: A review». In: *World Journal of Biology Pharmacy and Health Sciences* 12.03 (2022), pp. 039–053 (cit. on p. 11).

[27] Hyojin Ko et al. «A simple layer-stacking technique to generate biomolecular and mechanical gradients in photocrosslinkable hydrogels». In: *Biofabrication* 11 (2019) (cit. on p. 11).

[28] Enas M. Ahmed. «Hydrogel: Preparation, characterization, and applications: A review». In: *Journal of Advanced Research* 6.2 (2015), pp. 105–121. ISSN: 2090-1232 (cit. on p. 11).

[29] J.Y. Sun, X. Zhao, W. Illeperuma, et al. «Highly stretchable and tough hydrogels». In: *Nature* 489 (2012), pp. 133–136 (cit. on p. 12).

[30] Wei Seong Toh and Xian Jun Loh. «Advances in hydrogel delivery systems for tissue regeneration». In: *Materials Science and Engineering: C* 45 (2014), pp. 690–697. ISSN: 0928-4931 (cit. on p. 12).

[31] Nicholas A. Peppas, Y. Huang, M. Torres-Lugo, J. H. Ward, and J. Zhang. «Physicochemical foundations and structural design of hydrogels in medicine and biology». In: *Annual Review of Biomedical Engineering* 2 (2000), pp. 9–29 (cit. on pp. 12, 13).

[32] Yulia Berkovitch and Dror Seliktar. «Semi-synthetic hydrogel composition and stiffness regulate neuronal morphogenesis». In: *International Journal of Pharmaceutics* 523.2 (2017), pp. 545–555 (cit. on p. 14).

[33] A. Onaciu, R. A. Munteanu, A. I. Moldovan, C. S. Moldovan, and I. Berindan-Neagoe. «Hydrogels Based Drug Delivery Synthesis, Characterization and Administration». In: *Pharmaceutics* 11 (2019), p. 432 (cit. on p. 14).

[34] I. P. Harrison and F. Spada. «Hydrogels for Atopic Dermatitis and Wound Management: A Superior Drug Delivery Vehicle». In: *Pharmaceutics* 10 (2018), p. 71 (cit. on p. 14).

[35] Liangpeng Zeng, Xinxing Lin, Ping Li, Fa-Qian Liu, Hui Guo, and Wei-Hua Li. «Recent advances of organogels: from fabrications and functions to applications». In: *Progress in Organic Coatings* 159 (2021), p. 106417 (cit. on pp. 14, 15).

[36] R. Parhi. «Cross-Linked Hydrogel for Pharmaceutical Applications: A Review». In: *Advanced Pharmaceutical Bulletin* 7.4 (2017), pp. 515–530 (cit. on pp. 15, 16, 18–20, 22).

[37] Todd R. Hoare and Daniel S. Kohane. «Hydrogels in drug delivery: Progress and challenges». In: *Polymer* 49.8 (2008), pp. 1993–2007 (cit. on pp. 15, 16, 18, 19).

[38] Qingliang Zhao and Lin Chen. «Integrated Optical Coherence Tomography and Deep Learning for Evaluating of the Injectable Hydrogel on Skin Wound Healing». In: *IntechOpen* (2023). DOI: 10.5772/intechopen.106006 (cit. on p. 16).

[39] Weikang Hu, Zijian Wang, Yu Xiao, Shengmin Zhang, and Jianglin Wang. «Advances in crosslinking strategies of biomedical hydrogels». In: *Biomaterials Science* 7 (2019), pp. 843–855 (cit. on pp. 16, 17, 19, 20, 23).

[40] M. Bustamante-Torres, D. Romero-Fierro, B. Arcentales-Vera, K. Palomino, H. Magaña, and E. Bucio. «Hydrogels Classification According to the Physical or Chemical Interactions and as Stimuli-Sensitive Materials». In: *Gels* 7.4 (Oct. 2021), p. 182 (cit. on pp. 17, 19, 22, 23).

[41] Y. You, J. Yang, Q. Zheng, N. Wu, Z. Lv, and Z. Jiang. «Ultra-stretchable hydrogels with hierarchical hydrogen bonds». In: *Scientific Reports* 10 (2020), pp. 1–8 (cit. on p. 18).

[42] T. Yoshimura, R. Yoshimura, C. Seki, and R. Fujioka. «Synthesis and characterization of biodegradable hydrogels based on starch and succinic anhydride». In: *Carbohydrate Polymers* 64 (2006), pp. 345–349 (cit. on p. 18).

[43] J. R. Choi, K. W. Yong, J. Y. Choi, and A. C. Cowie. «Recent Advances in Photo-Crosslinkable Hydrogels for Biomedical Applications». In: *BioTechniques* 66.1 (2019), pp. 40–53 (cit. on p. 20).

[44] R. F. Pereira and P. J. Bártolo. «3D Photo-Fabrication for Tissue Engineering and Drug Delivery». In: *Engineering* 1.1 (2015), pp. 90–112 (cit. on pp. 20, 21).

[45] B. D. Fairbanks, M. P. Schwartz, C. N. Bowman, and K. S. Anseth. «Photoinitiated polymerization of PEG-diacrylate with lithium phenyl-2,4,6-trimethylbenzoylphosphinate: polymerization rate and cytocompatibility». In: *Biomaterials* 30.35 (2009), pp. 6702–6707 (cit. on p. 21).

[46] Sigma-Aldrich. *Lithium phenyl-2,4,6-trimethylbenzoylphosphinate (Numero di catalogo 900889)*. Sigma-Aldrich Italia. URL: https://www.sigmaaldrich.com/IT/it/product/aldrich/900889 (cit. on p. 21).

[47] V. Miletic, P. Pongprueksa, J. De Munck, N. R. Brooks, and B. Van Meerbeek. «Monomer-to-polymer conversion and micro-tensile bond strength to dentine of experimental and commercial adhesives containing diphenyl(2,4,6-trimethylbenzoyl)phosphine oxide or a camphorquinone/amine photo-initiator system». In: *Journal of Dentistry* 41.10 (2013), pp. 918–926 (cit. on p. 21).

[48] Sigma-Aldrich. *Diphenyl(2,4,6-trimethylbenzoyl)phosphine oxide (Numero di catalogo 415952)*. Sigma-Aldrich Italia. URL: https://www.sigmaaldrich.com/IT/it/product/aldrich/415952 (cit. on p. 22).

[49] Shan Xia, Shixin Song, Fei Jia, and Guanghui Gao. «A flexible, adhesive and self-healable hydrogel based wearable strain sensor for human motion and physiological signal monitoring». In: *Journal of Materials Chemistry B* 7 (2019), pp. 4638–4648 (cit. on pp. 23–25).

[50] F. Pinelli, L. Magagnin, and F. Rossi. «Progress in hydrogels for sensing applications: a review». In: *Materials Today Chemistry* 17 (2020), p. 100317. ISSN: 2468-5194. DOI: 10.1016/j.mtchem.2020.100317 (cit. on p. 23).

[51] Qian Zhang, Qian Wang, Guangyu Wang, Zilu Zhang, Shan Xia, and Guanghui Gao. «Ultrathin and Highly Tough Hydrogel Films for Multifunctional Strain Sensors». In: *ACS Applied Materials Interfaces* 13.42 (2021), pp. 50411–50421. DOI: 10.1021/acsami.1c16109 (cit. on pp. 24, 25).

[52] Zixuan Wu, Xing Yang, and Jin Wu. «Conductive Hydrogel- and Organohydrogel† Based Stretchable Sensors». In: *ACS Applied Materials & Interfaces* 13.2 (2021), pp. 2128–2144. DOI: 10.1021/acsami.0c19889 (cit. on pp. 24, 25).

[53] Ulrike Schmidt, Carola Jorsch, Margarita Guenther, and Gerald Gerlach. «Biochemical piezoresistive sensors based on hydrogels for biotechnology and medical applications». In: *Journal of Sensors and Sensor Systems* 5 (2016), pp. 409–417 (cit. on pp. 25, 26).

[54] Wufan Chen and Xin Yan. «Progress in achieving high-performance piezoresistive and capacitive flexible pressure sensors: A review». In: *Journal of Materials Science & Technology* 43 (2020), pp. 175–188. DOI: 10.1016/j.jmst.2019.12.012 (cit. on pp. 26–28).

[55] Margarita Guenther, Thomas Wallmersperger, and Gerald Gerlach. «Piezoresistive Chemical Sensors Based on Functionalized Hydrogels». In: *Chemosensors* 2.3 (2014), pp. 145–170. DOI: 10.3390/chemosensors2030145 (cit. on p. 26).

[56] Funian Mo, Yan Huang, Qing Li, Zifeng Wang, Ruijuan Jiang, Weiming Gai, and Chunyi Zhi. «A Highly Stable and Durable Capacitive Strain Sensor Based on Dynamically Super-Tough Hydro/Organo-Gels». In: *Advanced Functional Materials* 31 (2021). URL: https://api.semanticscholar.org/CorpusID:235509849 (cit. on p. 27).

[57] O. Young Kweon, Suman Kalyan Samanta, Yousang Won, Jong Heun Yoo, and Joon Hak Oh. «Stretchable and Self-Healable Conductive Hydrogels for Wearable Multimodal Touch Sensors with Thermoresponsive Behavior.» In: *ACS applied materials & interfaces* (2019). URL: https://api.semanticscholar.org/CorpusID:195845004 (cit. on p. 27).

[58] Yin Chen, Yiwen Xu, Qian Gao, Haisheng Qian, and Runhuai Yang. «Fabrication of Wearable Hydrogel Sensors With Simple Ionic-Digital Conversion and Inherent Water Retention». In: *IEEE Sensors Journal* 21 (2021), pp. 6802–6810. URL: https://api.semanticscholar.org/CorpusID:229657596 (cit. on p. 27).

[59] Yuxuan Du, Wenya Du, Dabin Lin, Minghao Ai, Songhang Li, and Lin Zhang. «Recent Progress on Hydrogel-Based Piezoelectric Devices for Biomedical Applications». In: *Micromachines* 14 (2023). URL: https://api.semanticscholar.org/CorpusID:255680053 (cit. on p. 28).

[60] Peng Fan, Hengwei Fan, and Shige Wang. «From emerging modalities to advanced applications of hydrogel piezoelectrics based on chitosan, gelatin and related biological macromolecules: A review.» In: *International journal of biological macromolecules* (2024), p. 129691. URL: https://api.semanticscholar.org/CorpusID:267218484 (cit. on p. 28).

[61] Yongzhi Liang, Lina Ye, Xingyue Sun, Qiong Lv, and Haiyi Liang. «Tough and Stretchable Dual Ionically Cross-linked Hydrogel with High Conductivity and Fast-Recovery Property for High-Performance Flexible Sensors.» In: *ACS applied materials & interfaces* (2019). URL: https://api.semanticscholar.org/CorpusID:208622263 (cit. on p. 29).

[62] Bowen Yang and Weizhong Yuan. «Highly Stretchable and Transparent Double-Network Hydrogel Ionic Conductors as Flexible Thermal-Mechanical Dual Sensors and Electroluminescent Devices.» In: *ACS applied materials & interfaces* 11 18 (2019), pp. 16765–16775. URL: https://api.semanticscholar.org/CorpusID:115199898 (cit. on pp. 29, 30).

[63] Xiaobin Li, Ending Zhang, Jun Shi, Xiaoyan Xiong, Jiaming Lin, Qiang Zhang, Xiaohua Cui, Liqin Tan, and Kun Wu. «Waterborne Polyurethane Enhanced, Adhesive, and Ionic Conductive Hydrogel for Multifunctional Sensors.» In: *Macromolecular rapid communications* (2021), e2100457. URL: https://api.semanticscholar.org/CorpusID:238859124 (cit. on p. 29).

[64] Chen-Jung Lee, Haiyan Wu, Yang Hu, Megan Young, Huifeng Wang, Dylan Lynch, Fujian Xu, Hongbo Cong, and Gang Cheng. «Ionic Conductivity of Polyelectrolyte Hydrogels». In: *ACS Applied Materials & Interfaces* 10.6 (2018). PMID: 29384644, pp. 5845–5852. DOI: 10.1021/acsami.7b15934 (cit. on p. 30).

[65] M. Vigata, C. Meinert, S. Pahoff, N. Bock, and D. W. Hutmacher. «Gelatin Methacryloyl Hydrogels Control the Localized Delivery of Albumin-Bound Paclitaxel». In: *Polymers* 12.3 (2020), p. 501. DOI: 10.3390/polym12030501 (cit. on p. 31).